PNNL-25303

Pacific Northwest
NATIONAL LABORATORY

Proudly Operated by Battelle *Since 1965*

Use of a Ca-Citrate-Phosphate Solution to Form Hydroxyapatite for Uranium Stabilization of Old Rifle Sediments: Laboratory Proof of Principle Studies

March 2016

JE Szecsody
RC Moore
MJ Rigali
VR Vermeul
J Luellen

U.S. DEPARTMENT OF ENERGY

Prepared for the U.S. Department of Energy
under Contract DE-AC05-76RL01830

DISCLAIMER

This report was prepared as an account of work sponsored by an agency of the United States Government. Neither the United States Government nor any agency thereof, nor Battelle Memorial Institute, nor any of their employees, makes **any warranty, express or implied, or assumes any legal liability or responsibility for the accuracy, completeness, or usefulness of any information, apparatus, product, or process disclosed, or represents that its use would not infringe privately owned rights**. Reference herein to any specific commercial product, process, or service by trade name, trademark, manufacturer, or otherwise does not necessarily constitute or imply its endorsement, recommendation, or favoring by the United States Government or any agency thereof, or Battelle Memorial Institute. The views and opinions of authors expressed herein do not necessarily state or reflect those of the United States Government or any agency thereof.

PACIFIC NORTHWEST NATIONAL LABORATORY
operated by
BATTELLE
for the
UNITED STATES DEPARTMENT OF ENERGY
under Contract DE-AC05-76RL01830

Printed in the United States of America

Available to DOE and DOE contractors from the
Office of Scientific and Technical Information,
P.O. Box 62, Oak Ridge, TN 37831-0062;
ph: (865) 576-8401
fax: (865) 576-5728
email: reports@adonis.osti.gov

Available to the public from the National Technical Information Service
5301 Shawnee Rd., Alexandria, VA 22312
ph: (800) 553-NTIS (6847)
email: orders@ntis.gov <http://www.ntis.gov/about/form.aspx>
Online ordering: http://www.ntis.gov

This document was printed on recycled paper.
(8/2010)

PNNL-25303

Use of a Ca-Citrate-Phosphate Solution to Form Hydroxyapatite for Uranium Stabilization of Old Rifle Sediments: Laboratory Proof of Principle Studies

JE Szecsody[1]
RC Moore[2]
MJ Rigali[2]
VR Vermeul[1]
J Luellen[3]

[1]Pacific Northwest National Laboratories, Richland, WA
[2]Sandia National Laboratories, Albuquerque, NM
[3]AECOM, Denver, CO

March 2016

Prepared for
the U.S. Department of Energy
under Contract DE-AC05-76RL01830

Pacific Northwest National Laboratory
Richland, Washington 99352

Summary

The Old Rifle Site is a former vanadium and uranium ore-processing facility located adjacent to the Colorado River and approximately 0.3 miles east of the city of Rifle, CO. The former processing facilities have been removed and the site uranium mill tailings are interned at a disposal cell north of the city of Rifle. However, some low level remnant uranium contamination still exists at the Old Rifle site. In 2002, the United States Nuclear Regulatory Commission (US NRC) concurred with United States Department of Energy (US DOE) on a groundwater compliance strategy of natural flushing with institutional controls to decrease contaminant concentrations in the aquifer. In addition to active monitoring of contaminant concentrations, the site is also used for DOE Legacy Management (LM) and other DOE-funded small-scale field tests of remediation technologies.

The purpose of this laboratory scale study was to evaluate the effectiveness of a hydroxyapatite ($Ca_{10}(PO_4)_6(OH)_2$) permeable reactive barrier and source area treatment in Old Rifle sediments. Phosphate treatment impact was evaluated by comparing uranium leaching and surface phase changes in untreated to PO_4-treated sediments. The impact of the amount of phosphate precipitation in the sediment on uranium mobility was evaluated with three different phosphate loadings. A range of flow velocity and uranium concentration conditions (i.e., uranium flux through the phosphate-treated sediment) was also evaluated to quantify the uranium uptake mass and rate by the phosphate precipitate.

Phosphate treatment decreased the mass and rate of uranium leached from the sediment in direct proportion to the amount of phosphate precipitated. While low phosphate treatment decreased uranium leached mass from the sediment by 40 to 70% and had little effect on the aqueous uranium, high phosphate treatment decreased uranium leached mass from the sediment by 100% and removed as much as 77% of aqueous uranium flowing through the PO_4 treated sediment. For an effective source area application, a phosphate loading of 3 mg PO_4/g of sediment or more was needed. For permeable reactive barrier application, a higher phosphate loading of 6 mg PO_4/g of sediment (highest phosphate loading tested) was needed to achieve continuous removal of 77% of the aqueous uranium. The rate of uranium removal by phosphate precipitate was ~5 to 35 μg U/Kg sediment/day, hence the PO_4-treated sediment was effective at low aqueous uranium concentration (32.1 μg/L) and natural Old Rifle groundwater flow rates (0.3 ft/day), but was less effective at higher uranium concentrations and flow rates.

The Old Rifle sediment used contained 1.39 ± 0.11 μg U/g of sediment, which was 7.4% aqueous and adsorbed, 56.3% carbonate associated, and 36.2% in oxide, sulfide, silicate, and other hard to extract phases, based on six sequential liquid extractions. Leaching the untreated sediments mobilized 53% to 64% of the uranium, which was mainly carbonate-associated and adsorbed uranium, whereas hard to extract phases were not mobilized. The phosphate treatment resulted in an increase in the oxide and hard to extract uranium phases (0.49 to 0.69 μg/g) compared to untreated sediment (0.47 μg/g), which accounts for the dramatic decrease in leaching. A phosphate precipitate formed during one treatment was identified as brushite ($CaHPO_4 \cdot 2H_2O$), which contained significant uranium (460 μg U/g) that was not adsorbed but co-precipitated in an unidentified uranium phase. Although the mechanism by which the phosphate treatment is removing uranium has not been positively identified, evidence that points toward formation of a U-PO_4 precipitate includes: a) increase in U uptake rate with higher PO_4 concentration, b) no change in adsorbed uranium for PO_4-treated sediments, c) no increase in U K_d for PO_4-treated sediments, and d) uptake of aqueous uranium from influent water. These multiple lines of evidence are consistent with (but do not prove) that the formation of a U-PO_4 precipitate (such as autunite) and not sorption or coating by a non-uranium phosphate precipitate exerts significant control in reducing uranium leaching from both sediment (i.e., source area treatment) and in aqueous solution (i.e., permeable reactive barrier treatment).

Overall, these results demonstrate that sufficient phosphate treatment of the sediment can be a viable remediation strategy for source area treatment of uranium, and under higher phosphate loading and/or low uranium flux, as a permeable reactive barrier. Additional laboratory scale experiments could further optimize the phosphate treatment and provide information to measure or predict the longevity. These experiments include: a) identification of uranium surface phases (to predict longevity), b) quantification of the optimal PO_4 mass needed for PRB application, c) quantification of Ca-citrate-PO_4 treatment under varied redox conditions (present at the Old Rifle site), and d) measurement of the long-term performance of the PO_4-treated sediments (ended at 90-140 pore volumes) to 500 to 1000 pore volumes.

Acknowledgments

Funding for this study was provided by the U.S. Department of Energy, Office of Legacy Management, Uranium Mill Tailings Radiation Control Act (UMTRCA) Program, managed by Richard Bush in the Grand Junction, Colorado office.

Definitions

adsorbed Ca^{2+}	Ca^{2+} held on the sediment surface by ion exchange to negatively charged minerals such as clays montmorillonite, illite, and others
apatite	Ca-phosphate precipitate, $Ca_{10}(PO_4)_6(OH)_2$, also known as hydroxyapatite
Ca-citrate PO_4 solution	an injection solution of Ca-citrate and Na-phosphates injected into Old Rifle sediments, which, after citrate biodegradation within 10s to 100s of hours, will precipitate amorphous Ca-PO_4 that recrystallizes into apatite after months
Ca-citrate-PO_4 depleted in Ca	an injection solution of Ca-citrate and Na-phosphates that has significantly less calcium than needed for phosphate precipitate (Ca/PO_4 molar ratio of 1.66), as adsorbed Ca^{2+} is also used as a Ca^{2+} source
Ca/PO_4 ratio	molar ratio of calcium to phosphate in precipitates, which varies from 1:1 for mono Ca-PO_4 to 1.66:1 for apatite (See Section 2.4 for details.)
EXAFS	Extended X-Ray Absorption Fine Structure
ICP-MS	inductively coupled plasma – mass spectrometer
KPA	laser-induced kinetic phosphorimetry measurement of aqueous U^{VI} (See Section 3.2.)
net uranium release mass	the mass of uranium released from leaching experiments as measured by the cumulative effluent mass minus the cumulative influent mass
leaching experiments	experiments in which groundwater is injected into a 1-D column filled with Old Rifle sediment for 10s to 1000s of hours. The effluent liquid is monitored for uranium, phosphate, and other constituents (See Section 3.3.)
LM	Legacy Management
PRB	permeable reactive barrier
SAT	source area treatment
U^{VI} (aq)	the total aqueous U^{VI} concentration, which is actually composed of one or more aqueous uranium complexes (See Section 2.2 for species details.)
uranium extractions	a series of six liquids added to sediment sequentially to remove different uranium surface phases from the sediment (See Section 3.2.)
uranium release mass	the mass of uranium released from leaching experiments, as measured by the cumulative effluent mass. This mass is composed of uranium released from the sediment as well as uranium injected into the leaching experiment.
uranium release rate	the rate of change of uranium mass in aqueous solution caused by contact with PO_4-treated sediment (in μg U^{VI}/g sediment/day)
US DOE	United States Department of Energy
US NRC	United States Nuclear Regulatory Commission
XANES	X-ray Absorption Near Edge Structure

Contents

Summary iii
Acknowledgments v
Definitions vii
1.0 Introduction 1
2.0 Background 1
2.1 Description of the Old Rifle Site 1
2.2 Uranium Aqueous Speciation and Expected Sorption Behavior 4
2.3 Phosphate Treatment Longevity and Uranium Surface Phase Identification 4
2.4 Ca-Citrate-Phosphate Injection Technology 5
3.0 Materials and Methods 6
3.1 Sediments and Solutions 6
3.2 Batch Uranium Extraction Experiments 7
3.3 1-D Column Leaching Experiments 7
4.0 Results 9
4.1 Uranium Leaching with PO_4 Treatment at 32 μg/L U Influent 9
4.2 Uranium Leaching with PO_4 Treatment at 179 or 383 μg/L U Influent 11
4.3 Changes in Uranium Surface Phases 13
4.4 Phosphate Precipitation Loading in the Sediment 15
4.5 Uranium Leaching and Uptake Rate in Untreated and PO_4-Treated Sediments 16
4.6 Uranium Sorption 17
5.0 Discussion 18
5.1 PO_4 Treatment and Source Area Stabilization: Sediment Uranium Mobility 18
5.2 PO_4 Treatment for Permeable Reactive Barrier: Aqueous Uranium Mobility 19
5.3 Phosphate Loading Effect on Uranium Uptake Mass and Rate 21
6.0 Summary and Recommendations 23
7.0 References Cited 24
Appendix A 1-D Column Individual Experiment Results A.1
Appendix B Uranium Extraction Results B.1
Appendix C Comparison of Leaching Results C.1
Appendix D Uranium Release Rates and Phosphate Concentration D.1
Appendix E Phosphate Concentration and U Mobility E.1

Figures

Figure 1. Map Showing the Location of the Old Rifle Site near Rifle, Colorado (US DOE 1999). 2

Figure 2. Arial Photograph of the Old Rifle Site Taken in 2013. 2

Figure 3. Old Rifle Site Experimental Station in 2015 Located in the Trailer in the Foreground.....3

Figure 4. Selected 1-D Leaching Columns Conducted with 32.1 μg/L Uranium Influent Concentration. a) U(VI) effluent concentration for untreated sediment, b) cumulative effluent uranium for untreated sediment, c) U(VI) effluent concentration for PO_4-treated sediment, and d) cumulative effluent uranium for PO_4-treated sediment.....10

Figure 5. 1-D Leaching Columns Conducted with 179 μg/L Uranium Influent Concentration. a) U(VI) effluent concentration for untreated ediment, b) cumulative effluent uranium for untreated sediment, c) U(VI) effluent concentration for PO_4-treated sediment, and d) cumulative effluent uranium for PO_4-treated sediment. Note that in both experiments, the injection concentration was changed to 383 μg/L in the last third of the experiment. 12

Figure 6. Comparison of Uranium Leaching Results for Columns Conducted with 32.1 μg/L Uranium Influent Concentration. a) Effluent U(VI) Concentration, and b) Cumulative Leached mass. 13

Figure 7. Uranium Extractions for a) Untreated Sediments, and b) PO_4-Treated Sediments. Leached represents net leached from sediment (effluent – influent). 14

Figure 8. X-Ray Diffraction Results of Precipitate in an Effluent Sample from a Phosphate-Treated Sediment (Experiment C59) in Black with Pattern of Brushite ($CaHPO_4 \cdot 2H_2O$) in Red. 15

Figure 9. Uranium Sorption Based on U(VI) Breakthrough Data and Phosphate Loading.....18

Figure 10. Uranium Cumulative Effluent Minus Influent in Leaching Experiments for Untreated and PO_4-Treated Old Rifle Sediments. 18

Figure 11. Uranium Effluent Concentrations with 32.1 μg/L Influent and Velocity of a) 0.28 ft/day, b) 0.84 ft/day, and c) 2.8 ft/day. 20

Figure 12. Uranium Release or Uptake Rate as a Function of Groundwater Velocity. Rates calculated from continuous flow data. 21

Figure 13. Phosphate Treatment Effect on a) Uranium Release or Uptake Rate, and b) Net Leached U Mass. 22

Tables

Table 1. Sediment Physical Properties in 1-D Columns 6
Table 2. Ca-Citrate-Phosphate Injection Solution 7
Table 3. 1-D Column Experiment Parameters 8
Table 4. Uranium Mass Balance in 1-D Columns 11
Table 5. Uranium Extraction Summary 14
Table 6. Phosphate Loading in Sediment Columns 16
Table 7. Uranium Release Rates During Continuous Flow 16
Table 8. Uranium Release Rates During Stop-Flow Events. 17
Table 9. Uranium Release Rates During Stop-Flow Events 17
Table 10. Phosphate Treatment Effectiveness 21

1.0 Introduction

The purpose of this study is to conduct an initial evaluation to assess the effectiveness of a hydroxyapatite ($Ca_{10}(PO_4)_6(OH)_2$) permeable reactive barrier and source area treatment to decrease uranium mobility at the Department of Energy (DOE) former Old Rifle uranium mill processing site in Rifle, western Colorado. Uranium mobility change as a result of the phosphate treatment was evaluated by: a) comparing uranium leaching in untreated to PO_4-treated sediments, b) comparing uranium present in multiple surface phases pre- and post-treatment using a series of six sequential uranium extractions, and c) surface phase analysis of the phosphate precipitate. Results of this study show both changes in uranium leaching from the sediment (i.e., source area treatment application), and changes in uranium uptake by the PO_4-laden sediment (i.e., permeable reactive barrier application).

2.0 Background

2.1 Description of the Old Rifle Site

The following section is a summary of the description of the Old Rifle Site compiled by Moore and Rigali (2015).

The Old Rifle Site is a former vanadium and uranium ore-processing facility located adjacent to the Colorado River and approximately 0.3 miles east of the city of Rifle, CO (Figure 1 and Figure 2). Union Carbide Corporation and its predecessor, the United States Vanadium Corporation, owned the Old Rifle Mill and operated it from 1924 to 1932 and again from 1942 to 1958. It processed vanadium ore during both operating periods and uranium ore only during the latter operating period. The former processing facilities have been removed and the site uranium mill tailings are interned at a disposal cell located in Estes Gulch, about 6 miles north of the city of Rifle. There is, however, some low level remnant uranium contamination at the Old Rifle site. In 2002, the United States Nuclear Regulatory Commission (US NRC) concurred with United States Department of Energy (US DOE) on a groundwater compliance strategy of natural flushing with institutional controls to decrease contaminant concentrations in the aquifer. In addition to active monitoring of contaminant concentrations, the site is also used for DOE Legacy Management (LM) and other DOE-funded small-scale field tests of remediation technologies.

Figure 2 is an aerial photograph of the Old Rifle Site taken in 2013. The site is bordered by a road to the west and the Colorado River to the east. The site is relatively small and hosts a 100 m by 100 m area for performing field tests. Access to the site is by dirt road which connects to the adjacent roadway. A trailer, not observable in the aerial photograph, but shown below (Figure 3), now sits on the site and houses analytical equipment for the site experimental program. There are several experimental well galleries that are located in front of and behind the trailer. The site has electrical power and a water treatment facility is located just to the north of the site where potable water can be obtained.

Groundwater levels at the site range from approximately 10 to 20 feet deep and rising about 5 to 6 ft. in late spring and early summer months in response to high Colorado River levels due to snowmelt runoff. In addition to causing temporary changes in groundwater flow directions, the seasonal high-water levels potentially rise to access uranium that would normally reside in the vadose zone. In addition, it is possible that there is infiltration and downward percolation of rainfall and snowmelt occurring on the site that could leach vadose zone contaminants including uranium prior to recharging the aquifer (US DOE 2012).

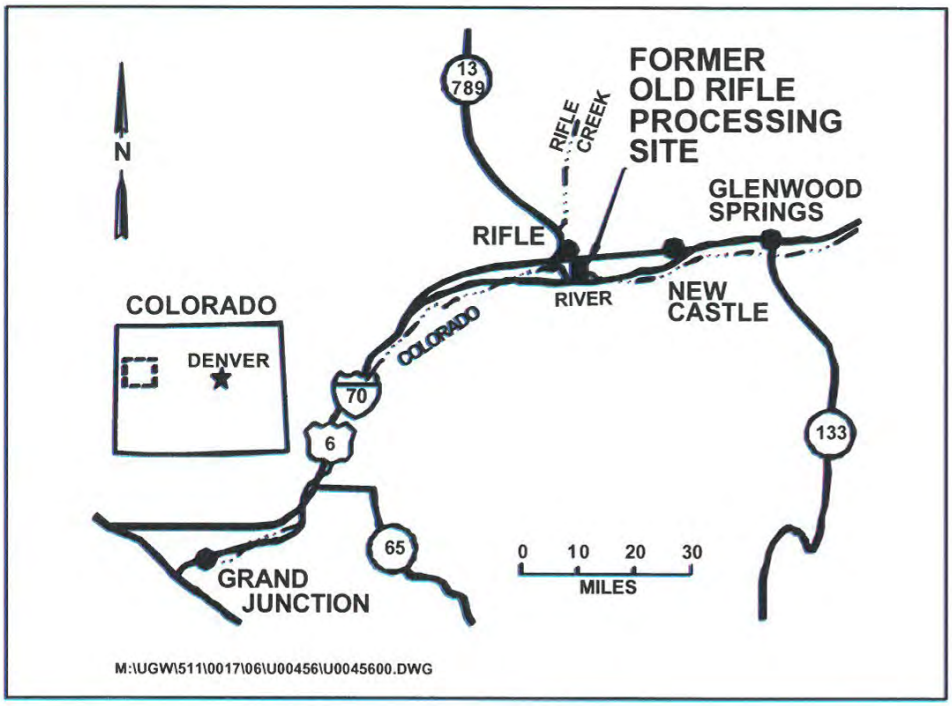

Figure 1. Map Showing the Location of the Old Rifle Site near Rifle, Colorado (US DOE 1999).

Figure 2. Arial Photograph of the Old Rifle Site Taken in 2013.

Figure 3. Old Rifle Site Experimental Station in 2015 Located in the Trailer in the Foreground.

The specific conductance of alluvial aquifer groundwater varies from about 1,800 to 5,000 microsiemens per centimeter (µS/cm), and is reflective of the total dissolved solid concentrations that vary between 1,500 to 4,500 mg/L (US DOE 1999). Alkalinity concentrations typically range between 300 to 600 mg/L as calcium carbonate and are indicative of relatively high dissolved bicarbonate concentrations. Dissolved nitrate levels are low; typically less than 2 mg/L. Sulfate concentrations, which commonly vary between 500 and 2,000 mg/L, are elevated ostensibly as a result of past milling activity at the site. The pH of the groundwater is near neutral to slightly basic (6.8 to 8.5). The redox state of the alluvial groundwater is manifested in a variety of chemical indicators. Most horizons within the saturated zone are exhibit dissolved oxygen concentrations of less than 0.3 mg/L (U.S. DOE 1999), signifying that anoxic conditions prevail. Meanwhile, the dissolved oxygen concentrations in the shallowest parts of the saturated zone have values as high as 2 to 2.5 mg/L. In addition, DO concentrations show a tendency to increase during periods of higher groundwater elevation (Yabusaki et al. 2007) in late spring and early summer. Dissolved iron concentrations range, from 0.003 mg/L to as high as 3 mg/L and averaging near 0.5 mg/L while aqueous manganese concentrations as high as 2 mg/L are common. Oxidation-reduction potential of the groundwater ranges from –250 millivolts (mV) to about 100 mV. In summary, these characteristics are representative of a slightly reducing environment and suggest that uranium has the potential to flush naturally (US DOE 1999).

Uranium-contaminated sediments in the vadose and saturated zones at the site are the source of elevated U(VI)concentrations (0.2–1.2 mM) presently observed in groundwater. Groundwater flows through unconsolidated Quaternary flood plain deposits that are composed mainly of quartz and feldspar, sands, plus silts, clays, pebbles, and cobbles (US DOE 1999; Hyun et al. 2009; Komlos et al. 2008). The sediments are often observed to be coated with iron oxide minerals. Beneath the Quaternary sediments sits a relatively impermeable bedrock layer of the Tertiary Wasatch Formation. This bedrock occurs at an average depth of approximately 8 m.

In 2012 Campbell et al., performed a study of the Old Rifle Site with respect to redox conditions. The study reveals that there are localized zones of naturally reduced sediments are present and that these

sediments may play a significant role in the fate and transport of redox sensitive metals including uranium in the site aquifers. Solid-phase amounts of uranium as U(IV) were found to be higher in the naturally reduced zones. Increased concentration of solid-phase organic carbon and biomass in the naturally reduced sediment suggests that natural bioreduction is stimulated in these reduced zones and is responsible for elevated uranium concentrations in these areas.

Several features of the site make it ideal for use of the apatite forming solution technology for permeable reactive barrier (PRB) and source area treatment (SAT) injections. These include:

- The sediment at the site is fairly permeable and will allow the apatite forming fluids to flow and distribute well throughout the sediment;
- The pH of the ground water at the site varies between 6.9 and 7.8 and is optimal for apatite formation;
- The site groundwater flow rate is very low and should allow sufficient time for the PRB and SAT to set up;
- Additionally the slow groundwater flow rate will allow time for uranium to interact and be immobilized by the PRB;
- The site has been extensively characterized and there are a number of injection and monitoring wells in place in several well galleries;
- There is analytical equipment on site including inductively coupled plasma – mass spectrometer (ICP-MS) and ion chromatography.

2.2 Uranium Aqueous Speciation and Expected Sorption Behavior

Uranium sorption to sediment is highly dependent on pH and carbonate concentration. At the Hanford Site, subsurface pH is 7.5–8.0 in carbonate-saturated groundwater, U^{+6} species present are primarily $Ca_2UO_2(CO_3)_3$ (aq), $CaUO_2(CO_3)_3^{2-}$ (and to a lesser extent magnesium equivalent phases, Zachara et al., 2007; Liu et al. 2008), with smaller concentrations of $(UO_2)_2CO_3(OH)_3^-$ and $UO_2(CO_3)_2^{2-}$, which is likely similar to the Old Rifle Site (although it is important to note that there is higher carbonate concentration in the Old Rifle groundwater). Note also that although adsorption of uranium is assumed to be reversible, additional uranium-mineral phase interactions occur over time that more strongly retain U(VI) species (Smith and Szecsody et al. 2011; Bond et al. 2008).

The U(VI) sorption in Old Rifle sediments will vary with the specific mineralogy of the sediment. Aqueous carbonate concentration exerts major control on U(VI) adsorption, as most Ca-U-CO_3 species are dominant in this mid-pH range. An increase in ionic strength greater than groundwater may lead to some U(VI) species desorption due to competition for adsorption sites. The U(VI) species sorption is likely to be anionic (increasing sorption with lower pH) in the neutral to weakly alkaline Old Rifle sediments (pH 7–9), which is also representative of U(VI) species adsorption to major mineral phases (ferrihydrite, kaolinite, and quartz; Zachara et al. 2007).

2.3 Phosphate Treatment Longevity and Uranium Surface Phase Identification

Previous studies at the Hanford Site have provided some insight into both the longevity of the phosphate treatment as well as the identity of surface phases. Short term leaching experiments (total flow time of 350 h) of a high uranium-bearing-sediment (112 μg/g) showed that a 50 mM PO_4 treatment prevented uranium leaching for 200 pore volumes (Shi et al. 2009). In another study, long term (450 pore volumes

over 3000 h) showed 45 mM PO_4 treatment decreased uranium leaching from the sediment by 70% (Szecsody et al., 2012b).

In previous a phosphate treatment study (Shi et al. 2009) using a Hanford 200 Area BX sediment that contained considerably higher uranium concentration (112 μg/g), X-ray fluorescence spectroscopy showed an initial adsorption of uranium to phosphate precipitates followed by a slow transformation to multiple U-phosphate precipitates (Shi et al. 2009). In a separate study of phosphate treatment on a high concentration of uranium-bearing sediment, 14% of the uranium formed autunite, and the remaining uranium co-precipitated with calcite based on Extended X-Ray Absorption Fine Structure (EXAFS) data, (Wellman et al. 2008a, b, 2011, Vermeul et al., 2009). Although a hypothesized treatment process based on NH_3 gas treatment of U-contaminated sediment is completely different, a similar coating process could be occurring. In that study, ammonia gas treatment of a field-contaminated sediments containing 300 μg/g uranium from the Hanford Site, significant decrease in uranium leaching over 3 years (Zhong et al. 2015) was attributed to uranium-silicate surface phases being coated with low solubility phosphates, based on EXAFS and X-ray Absorption Near Edge Structure (XANES) analysis (Szecsody et al. 2012a). Identification of uranium surface phases in phosphate-treated sediments is possible with moderate to high uranium concentrations (> 50 μg/g), and likely not possible in sediments with low uranium concentration such as the Old Rifle site.

2.4 Ca-Citrate-Phosphate Injection Technology

The method of emplacing apatite in subsurface sediments is to inject or infiltration an aqueous solution containing a Ca-citrate complex and Na-phosphate (Moore et al. 2004, 2007). Phosphate adsorption is slow (hours) so injection or rapid infiltration can result in significant phosphate mass distribution. Citrate is needed to keep Ca in solution long enough (days) to accomplish the injection into the subsurface. In the absence of citrate a solution containing just Ca^{2+} and phosphate will rapidly form mono- and di-calcium phosphate [$Ca(H_2PO_4)_2$, $CaHPO_4*2H_2O$] (Andronescu et al. 2002; Elliot et al. 1973; Papargyris et al. 2002). The relatively slow biodegradation of the Ca-citrate complex in the subsurface (days) allows sufficient time for injection and transport of the reagents to the areas of the aquifer where treatment is required (Szecsody et al. 2009). As Ca-citrate is degraded (Van der Houwen and Valsami-Jones 2001; Misra 1998), the free Ca and phosphate combine to form amorphous precipitate. The formation of amorphous precipitate occurs within a week and crystalline apatite forms within a few weeks. Citrate biodegradation rates in Hanford 100-N sediments (water-saturated) at temperatures from 10°C to 21°C (aquifer temperature 15°C to 17°C) over the range of citrate concentrations to be used (10 mM to 100 mM) have been determined experimentally and simulated with a first-order model (Bailey and Ollis 1986; Bynhildsen and Rosswall 1997). In addition, the Hanford 100-N microbial biomass has been characterized with depth and within river water (used for injections), and the relationship between biomass and the citrate biodegradation rate determined. Because Hanford 100-N Area injections typically use river water (~90% to 95%) with concentrated chemicals, microbes in the river water are also injected, which results in a somewhat more uniform citrate biodegradation rate in different aquifer zones.

Emplacement of apatite precipitate by a solution injection/infiltration has significant advantages over other apatite emplacement technologies for application at the Old Rifle site. The major advantage is minimal disturbance of the subsurface (both vadose and saturated zone), as this technology only requires injection wells (for groundwater remediation) or a surface infiltration gallery (for vadose zone treatment), in contrast with excavation of the river bank for trench-and-fill emplacement of solid-phase apatite. Other apatite emplacement technologies were also considered for the 100-N Area (DOE-RL 2005), which included pneumatic injection of solid apatite and vertical hydrofracturing for apatite emplacement both as a permeable reactive barrier and grout curtain. Although each technology has advantages and

disadvantages, the Ca-citrate-PO_4 injection technology was chosen as it appears to provide the most economic emplacement methodology.

The original calcium-citrate-phosphate amendment formulation was based on the stoichiometric ratio of Ca:PO_4 in apatite (5:3), and a Ca:citrate ratio of 1:2.5 to form the aqueous Ca-citrate complex [6, 10]. Therefore, the initial Ca-citrate-PO_4 formulation contained the ratios of 4 mM Ca, 10 mM citrate, and 2.4 mM PO_4. Early laboratory experiments with this formulation (and higher concentrations) did successfully precipitate apatite, but left considerable excess Ca in solution. This is because there is a significant quantity of adsorbed Ca^{2+} on sediment minerals (by ion exchange) that exchanges off the mineral surface during solution injection [8]. Injection of any calcium-poor solution (i.e., less Ca than the 10:6 ratio of Ca:PO_4) will utilize some ion exchangeable Ca^{2+} from the sediment. However, it should be noted that not all calcium on ion exchange sites can be desorbed with the Ca-citrate-PO_4 injection solution, which contains primarily Na+. Overuse of calcium-poor Ca-citrate-PO_4 solutions will deplete the sediment Ca^{2+} content, and the unreacted phosphate would end up moving downgradient in the aquifer to a zone with some available calcium for precipitation to occur. The optimal concentration apatite amendment formulation designed to utilize some uranium in the initial precipitation and minimize the initial uranium peak from desorption was a Ca-citrate-PO_4 solution with a 1: 2.5:11 ratio, which is 95% depleted in the calcium needed to form apatite (i.e., 95% of the calcium used in apatite formation is desorbed from aquifer sediments). Optimization of the Ca-citrate-PO_4 solution formulation at other sites (such as Old Rifle) would require additional experimentation to evaluate: a) Ca^{2+} availability from ion exchange sites, b) in situ or injection water microbial biomass, and c) the rate of citrate biodegradation.

3.0 Materials and Methods

3.1 Sediments and Solutions

Sediment obtained from the Old Rifle Site from Ken Williams (Lawrence Berkley National Laboratory) was collected from a specific well (BH 2-1-13 < 4.74 mm) and was close to water saturated. The sediment was used in batch experiments (Section 3.2) and 1-D column leaching studies (Section 3.3). The average packed dry bulk density of the sediment in the six columns was 1.533 ± 0.063 cm3/g and porosity 0.394 ± 0.050 (Table 1).

Table 1. Sediment Physical Properties in 1-D Columns

#	dry sed. (g)	pore vol. (mL)	dry bulk density (g/cm3)	porosity (cm3/cm3)
C54	102.657	23.463	1.578	0.3606
C55	103.247	22.313	1.587	0.3430
C56	95.804	30.456	1.473	0.4681
C57	93.628	28.682	1.439	0.4408
C58	102.982	25.238	1.583	0.3879
C59	100.005	23.675	1.537	0.3639

Twenty liters of Old Rifle groundwater received from the site had a U(VI) concentration of 32.1 μg/L. This groundwater was used as the injection concentration in some experiments and in others additional U(VI) was added (as uranyl nitrate) to achieve concentrations of 178.9 or 383.4 μg/L. For phosphate injections, the 32.1 μg/L U(VI) groundwater was used and amendments were added (Table 2). Formation of apatite [$Ca_{10}(PO_4)_6(OH)_2$] requires significant calcium and phosphate at specific ratios at pH 7.5.

Previous studies in slightly alkaline high Ca,Mg-carbonate systems (i.e., Hanford Site, WA) have shown that calcium on ion exchange sites can be used (within limits) to supply most of the calcium, so rather than using a molar ratio of 10:6 ($Ca:PO_4$) required in the structure, a 1:9 ratio was optimized for work at the Hanford subsurface. The same formula was used for Old Rifle sediment injections. It should be pointed out that given the cation exchange capacity at in Hanford sediments (2 meq/100 g) and high calcium (i.e., 75% of the ion exchange sites had Ca), sufficient calcium could desorb and be utilized to precipitate 35 mM phosphate. A similar optimization process may be needed for the Old Rifle site, especially if high phosphate loadings are required.

Table 2. Ca-Citrate-Phosphate Injection Solution

Na_2HPO_4 (mM)	NaH_2PO_4 (mM)	NH_4HPO_4 (mM)	$CaCl_2$ (mM)	triNaCitrate (mM)	total PO_4 (mM)	pH
36.45	6.3	2.25	4.05	10.1	45.00	7.52

3.2 Batch Uranium Extraction Experiments

Sediment samples were analyzed for uranium on surfaces or precipitated as mineral phases using a series of six sequential liquid extractions. Uranium is present as predominantly aqueous $Ca_2UO_2(CO_3)_3$ aq, and $CaUO_2(CO_3)_3^{2-}$at pH 8 (Liu et al. 2008; Zachara et al. 2007). Uranium obtained from the first extraction (aqueous uranium) was extracted using natural groundwater. The second extraction (adsorbed uranium species) was done with a carbonate solution (0.0114 mol/L $NaHCO_3$, 0.0028 mol/L Na_2CO_3, 1 h, Smith and Szecsody et al. 2012a). Uranium is present in these natural and field-contaminated sediments in multiple precipitates including U-carbonates (liebigite, rutherfordine, and other coprecipitates with $CaCO_3$), hydrous silicates (Na-boltwoodite, uranophane), and harder to extract phases such as U-phosphates (Liu et al., 2008). An additional four sequential liquid extractions of increasing strength were used to characterize uranium mobility (i.e., harder to extract phases are less mobile). The following four extractant solutions used sequentially after the aqueous and adsorbed U extraction and include: a) extraction 3, 1 mol/L sodium acetate (pH 5. 1 h), b) acetic acid (pH 2.3, 5 days), c) extraction 4, 0.1 mol/L ammonium oxalate, c) extraction 5, 0.1 mol/L oxalic acid (1 h), and d) extraction 6, 8 mol/L HNO_3, 95°C, 2 h. For contaminated sediments, a portion (thin rind) of carbonates (possibly U-laden) are dissolved in the pH 5 acetate (extraction 3) solution. The remaining carbonates are dissolved in the 5 day acetic acid (extraction 4, pH 2.3, Kohler et al. 2004). Na-boltwoodite is predominantly dissolved in the acetic acid extraction. The oxalate extraction (extraction 5) dissolves primarily amorphous and crystalline oxides (Chao and Zhou 1983). The 8 mol/L hot nitric acid (extraction 6) dissolves additional hard to extract uranium phases, including phosphate preciptiates. Sediment total digestion for untreated sediments produces an additional 20% uranium, but the purpose of these six sequential extractions was to quantify phases that are potentially able to interact with pore water (i.e., aqueous, adsorbed, associated with carbonates, and in hydrous silicates). Aqueous uranium (as U(VI)) from extractions was measured by laser-induced kinetic phosphorimetry (KPA, Brina and Miller 1992).

3.3 1-D Column Leaching Experiments

Long-term 1-D column leaching experiments were conducted to evaluate the uranium release mass and rate from field-contaminated sediments. For these experiments, sieved material was packed into 2.35 cm diameter by 15-cm long stainless steel columns with 2-micron Teflon end frits. High performance liquid chromatography pumps were used to inject simulated groundwater upward through the column at a constant flow rate. Column experiments used 2 to 4 different constant flow rates, each for 100s of hours to evaluate the uranium uptake rate by the phosphate precipitate (Table 3). Flow rates ranged from 0.26

ft/day (similar to average groundwater flow at the Old Rifle Site) to 4.3 ft/day. The groundwater velocity from the Old Rifle field site averages about 0.3 ft/day, but varies seasonally. In addition, flow through the aquifer varies with low- and high- hydraulic conductivity layers and inclusions in the aquifer. Stop-flow events ranging from 16 to 960 h were also used in column experiments to further define the rate at which uranium leached off the untreated sediment, or was precipitated in the PO_4-treated sediment. In addition to different flow rates, the U(VI) concentration in the Old Rifle groundwater injected into the column was varied to evaluate the efficiency of the PO_4 precipitate to uptake differing U(VI) fluxes. The Old Rifle groundwater received from the site had 32.1 μg/L U(VI) concentration, and was used as the injection water in one untreated (C54, Table 2) and three PO_4-treated column experiments. Additional U(VI) was added to the groundwater to obtain 178.9 μg/L in an untreated and PO_4-treated column.

Table 3. 1-D Column Experiment Parameters

#	PO4 treatment	U(VI) inject conc. (ug/L)	Flow Rate (ft/day)
C55	none	178.85	4.27
		383.4	0.383
C56	1 x 45 mM	178.85	2.84
		383.4	0.258
C54	none	32.1	4.19
		32.1	0.371
C57	1 x 45 mM	32.1	3.46
		32.1	0.283
C58	2 x 45 mM	32.1	2.68
		32.1	0.822
		32.1	0.32
C59	4 x 45 mM	32.1	2.71
		32.1	0.813
		32.1	0.298

Thus, column experiments used a different flow rates, different U(VI) concentrations, and stop-flow events to obtain leaching data suitable to evaluate: a) U(VI) sorption, b) U(VI) leaching from the sediment (i.e., the PO_4 treatment as a source area treatment), and c) influent aqueous U(VI) uptake mass and rate (i.e., the PO_4 treatment as a permeable reactive barrier). Constant groundwater injection continued for 866 to 2928 h, with two to three stop-flow events. Effluent was collected using a fraction collector (Isco Foxy 200) and 0.45 μm filtered samples were analyzed at selected time intervals for U^{VI}, phosphate, specific conductance, and pH. For stop-flow events, the difference in U^{VI} concentrations and stop-flow time was used to calculate a rate of U^{VI} release from the sediment.

The Ca-citrate-phosphate injections into the sediment were conducted at a fast flow rate (~4 ft/day) for 15 pore volumes (single injections) to insure uniform phosphate precipitate in the column. The effluent phosphate concentration was measured to confirm the 45 mM PO_4 injection concentration was also in the effluent. The precipitation process (described in the introduction) takes 1 to 2 weeks to form initially amorphous Ca-PO_4 precipitate, which crystallizes into monocalcium phosphate, then di-calcium phosphate, then apatite over months. Following the Ca-citrate-phosphate injection, a stop-flow period of 700 to 950 h was used to allow for precipitation to occur. To evaluate the influence of phosphate mass on uranium uptake, additional phosphate precipitation was desired. The practical phosphate concentration limit in the injection solution of 60 mM has been previously injected, although theoretically 100 mM phosphate should not precipitate. High ionic strength solutions (relative to the native groundwater) cause some desorption of uranium, so higher phosphate loadings were achieved in this study by multiple

injections. For one sediment column, two injections of 45 mM PO_4 were injected (i.e., Table 3, C58, 2 x 45 mM) and in another sediment column four injections of 45 mM PO_4 were injected (Table 3, C59).

4.0 Results

4.1 Uranium Leaching with PO_4 Treatment at 32 μg/L U Influent

Old Rifle groundwater with 32.1 μg/L uranium was injected into one untreated and three PO_4-treated sediment columns to evaluate difference in uranium leaching from the sediment as well as change in the uranium injection concentration. The effluent in each column study was used to measure aqueous U(VI), pH, specific conductance, and phosphate (for PO4-treated columns). Uranium sequential extractions were conducted on the untreated Old Rifle sediment (in triplicate) and in the post-leach sediment for each column. Phosphate extractions were also conducted on the post-leach sediment. A comparison of one untreated and one phosphate-treated sediment (Figure 4) show significantly less uranium leaching from the PO_4-treated sediment. For the untreated sediment, there is a large uranium effluent spike initially (to 600 μg/L, Figure 4a), then over time the effluent uranium concentration decreases to an average of 43 μg/L, due to the 32.1 μg/L uranium influent concentration plus some additional uranium leaching off the sediment (i.e., from desorption and also dissolution of some U-carbonate phases, as described in Section 4.3). The pH breakthrough for untreated sediment (Appendix A, experiment C54) initially shows a pH of 7.6, and then equilibrates to 8.5 after a few pore volumes. This shift may indicate the sediment (as obtained) was not in equilibrium with the groundwater and may account for the large initial uranium spike. The specific conductance also decreased from 1600 to 1100 μS/cm. In contrast, the sediment column that received high phosphate treatment (Figure 4c and Figure 4d) shows an initial spike of 60 μg/L, then uranium concentrations trend at less than the 32 μg/L influent concentration. Experiments include changes in uranium concentrations due to stop-flow events and changes in velocity. A decrease in velocity (50 – 60 pore volumes) resulted in a lower U effluent concentration, and an increase in velocity (60 – 90 pore volumes) resulted in a higher U effluent concentration. The uranium uptake rate changed at the different velocities (Section 5.2, Figure 12).

Cumulative uranium effluent mass plots (Figure 4b and Figure 4d) also show significant differences between untreated and PO_4-treated sediments. For the untreated sediment, the cumulative effluent mass is greater than the influent mass, indicating influent uranium is flowing through the sediment and additional uranium is leaching from the sediment. There is significantly more uranium leaching initially (i.e., from the initial high concentration spike), but over time the effluent and influent slopes are similar by 130 pore volumes. In contrast, for the PO_4-treated sediment column, the effluent mass is less than the influent mass meaning uranium is not leaching from the sediment as well as there is a net uptake of uranium present in the influent. If the phosphate treatment only stabilized the uranium in the sediment and did not adsorb or precipitate any influent uranium, then the cumulative effluent mass would be equal to the influent mass (minus a slightly delay initially due to sorption). The rate of uranium uptake by PO_4-treated sediment was characterized during flow and during stop-flow events, and is described in detail in Section 5.3 below. The uranium mass balance (Table 4) shows the untreated sediment (experiment C54) leached 1.8 μg/g uranium (with 0.91 μg/g influent, or a net of 0.89 μg/g leached), and the high PO_4-treated sediment (experiment C59) net uptake was -0.337 μg/g. This means that no uranium was leached and that there was also additional uranium uptake from the influent. Sediments that received less phosphate treatment also leached less uranium compared with the untreated sediment (described in detail in Section 5.1). Two additional columns with groundwater injection at 32.1 μg/L uranium received lower phosphate treatment (Appendix A, experiments C57 and C58) and showed expected behavior (Section 4.2, Figure 6).

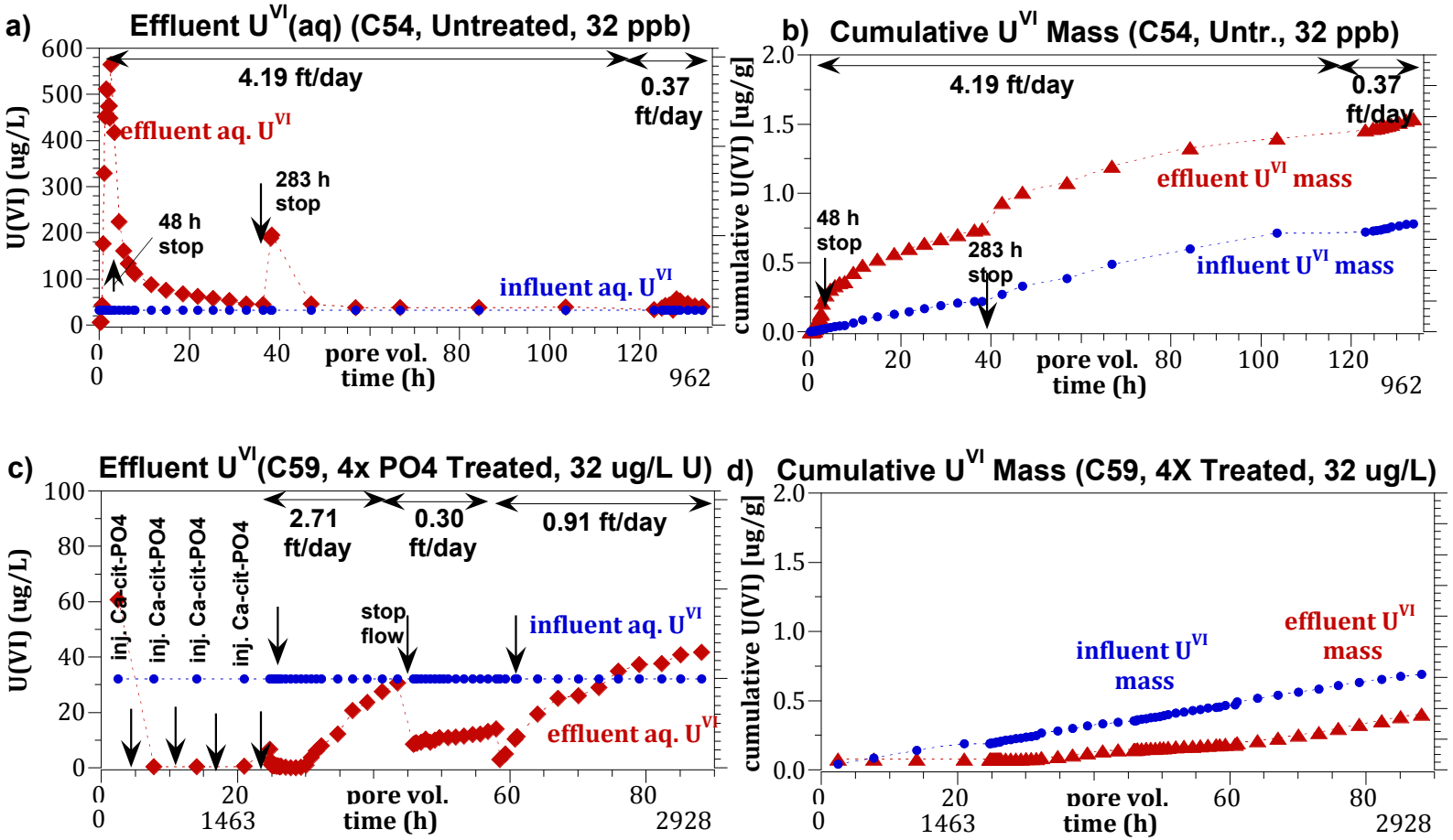

Figure 4. Selected 1-D Leaching Columns Conducted with 32.1 μg/L Uranium Influent Concentration: a) U(VI) effluent concentration for untreated sediment, b) cumulative effluent uranium for untreated sediment, c) U(VI) effluent concentration for PO_4-treated sediment, and d) cumulative effluent uranium for PO_4-treated sediment.

Comparisons of the amount of phosphate injected and influence on uranium mobility are in Section 5.1 and 5.2. The breakthrough data for all experiments are shown in Appendix A.

4.2 Uranium Leaching with PO_4 Treatment at 179 or 383 μg/L U Influent

To evaluate the influence of different uranium injection concentration on the performance of the PO_4-treated sediment, two additional column experiments were conducted in which groundwater with 178.9 or 383 μg/L uranium was injected into a untreated Old Rifle sediment column (Figure 5a and b, experiment C55) and PO_4-treated sediment (Figure 5c and d, experiment C56). For the untreated sediment, initial uranium breakthrough showed a high peak (490 μg/L, Figure 5a), similar to the previous untreated sediment (Figure 4a), but then the concentration leveled out slightly above the influent concentration of 179 μg/L. The cumulative uranium mass breakthrough (Figure 5b) showed effluent (in red) above influent (in blue). Stop-flow events showed an increase in uranium concentration, indicating uranium dissolution from surface phases. Uranium extractions characterizing changes in these surface phases (Section 4.3) showed that for the untreated sediment, 8% of the uranium is aqueous or adsorbed, 50% is associated with carbonate, and 42% associated with oxides, sulfides, or other hard to extract (i.e., less mobile) phases. Leaching the untreated sediment mobilized about 35% of the uranium, which included the aqueous, adsorbed, and most of the carbonate-associated uranium, leaving the oxide, sulfide, and hard to extract phases relatively intact. The total mass of uranium leached from the untreated sediment was 0.74 μg/g (Table 4, total leached minus influent), which was somewhat less than what was leached from the other untreated sediment column (0.89 μg/g) that had 32 μg/L uranium influent concentration.

Table 4. Uranium Mass Balance in 1-D Columns

#	PO4 treatment	U(VI) inject conc. (ug/L)	U(VI) Influent (ug/g)	U(VI) effluent (ug/g)	Net Leached U(VI) (ug/g)
C55	none	179, 383	7.611	8.345	0.735
C56	1 x 45 mM	179, 383	6.709	6.928	0.220
C54	none	32.1	0.907	1.800	0.893
C57	1 x 45 mM	32.1	1.074	1.610	0.536
C58	2 x 45 mM	32.1	0.750	0.748	-0.002
C59	4 x 45 mM	32.1	0.804	0.467	-0.337

* + is U release from sed., - is U uptake by sed.

In contrast, the sediment, which received a low (i.e., single 45 mM PO_4) phosphate treatment, leached considerably less uranium than the untreated sediment. The effluent concentration peaked at 290 μg/L (Figure 5c). During stop-flow events, the uranium concentration actually decreased upon restart (see 145 h stop flow at 50 pore volumes in Figure 5c), indicating uranium uptake by the phosphate precipitate. The net amount of uranium leached from this PO_4-treated sediment was 0.22 μg/g (Table 4, experiment C56), or considerably less than the 0.74 μg/g for the untreated sediment. While even the low phosphate treatment was effective at reducing uranium mobility of the uranium surface phases (i.e., source area application), the high uranium influent was poorly treated. Therefore, the ratio of phosphate loading in the sediment to uranium total flux influences performance as both source area treatment and a permeable reactive barrier. High phosphate treatment with low uranium flux (i.e., experiment C59, Figure 4c and d) performed well as a PRB and source area application, whereas low phosphate treatment with high uranium flux (i.e., experiment C56, Figure 5c and d) performed well for source area treatment but less effectively as a PRB (discussed further in Section 4.4).

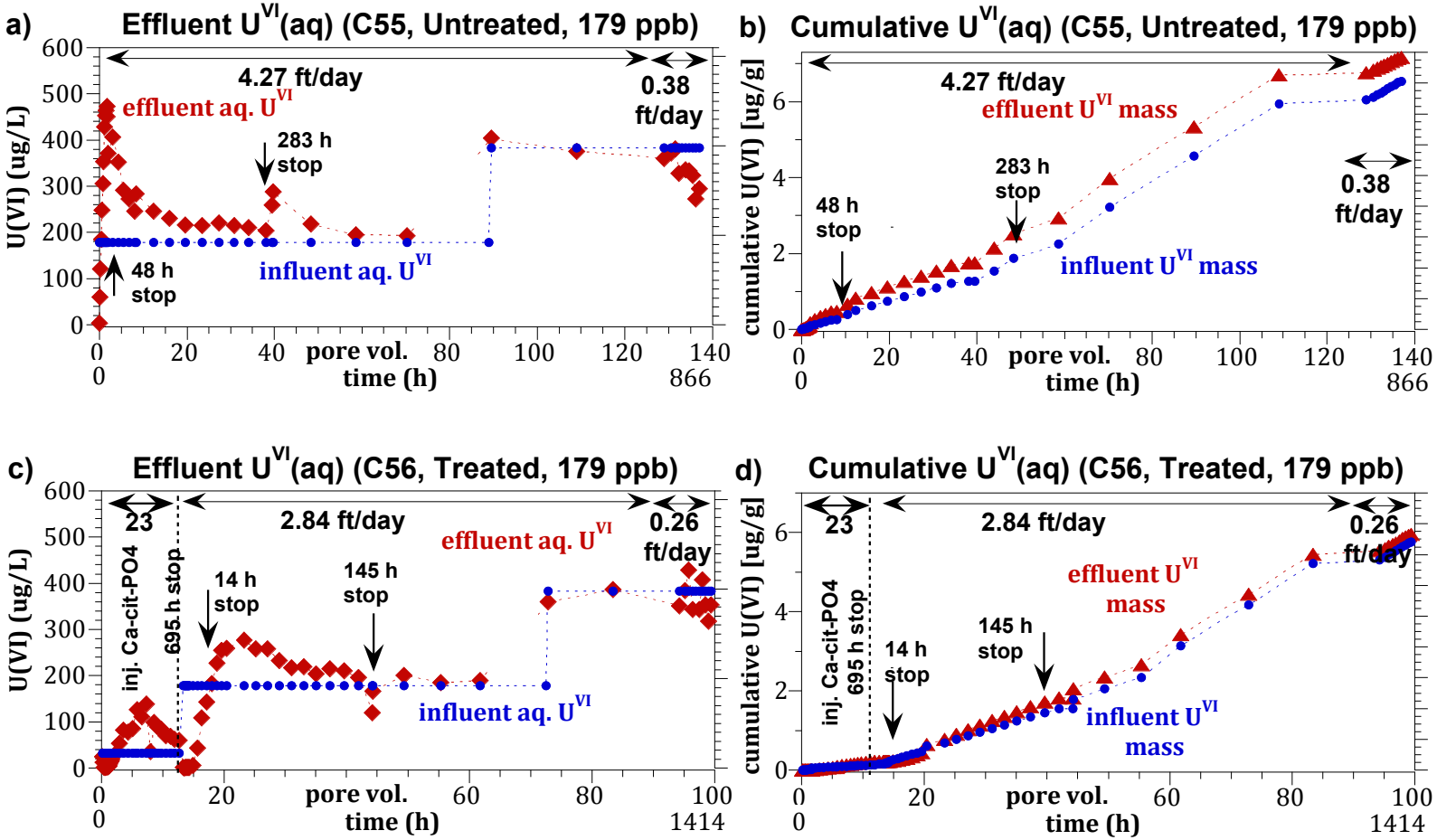

Figure 5. 1-D Leaching Columns Conducted with 179 μg/L Uranium Influent Concentration: a) U(VI) effluent concentration for untreated ediment, b) cumulative effluent uranium for untreated sediment, c) U(VI) effluent concentration for PO_4-treated sediment, and d) cumulative effluent uranium for PO_4-treated sediment. Note that in both experiments, the injection concentration was changed to 383 μg/L in the last third of the experiment.

A single graph illustrating effluent concentrations of all four columns with 32.1 μg/L uranium influent (one untreated, three phosphate treated) clearly shows lower and lower uranium effluent concentrations with increasing phosphate treatment (Figure 6a). In addition, a comparison of the cumulative effluent concentrations shows the dramatic decrease in uranium leaching from the sediment and also from the influent with higher phosphate treatment (Figure 6b). It should be noted that this cumulative leached uranium (Figure 6b) is total effluent, whereas the net uranium leached from the sediment (i.e., total effluent minus influent) is described in Section 5.1. The data are presented in this fashion in order to separate how much effluent uranium is mobilized from the sediment in the column and how much is sourced from the influent.

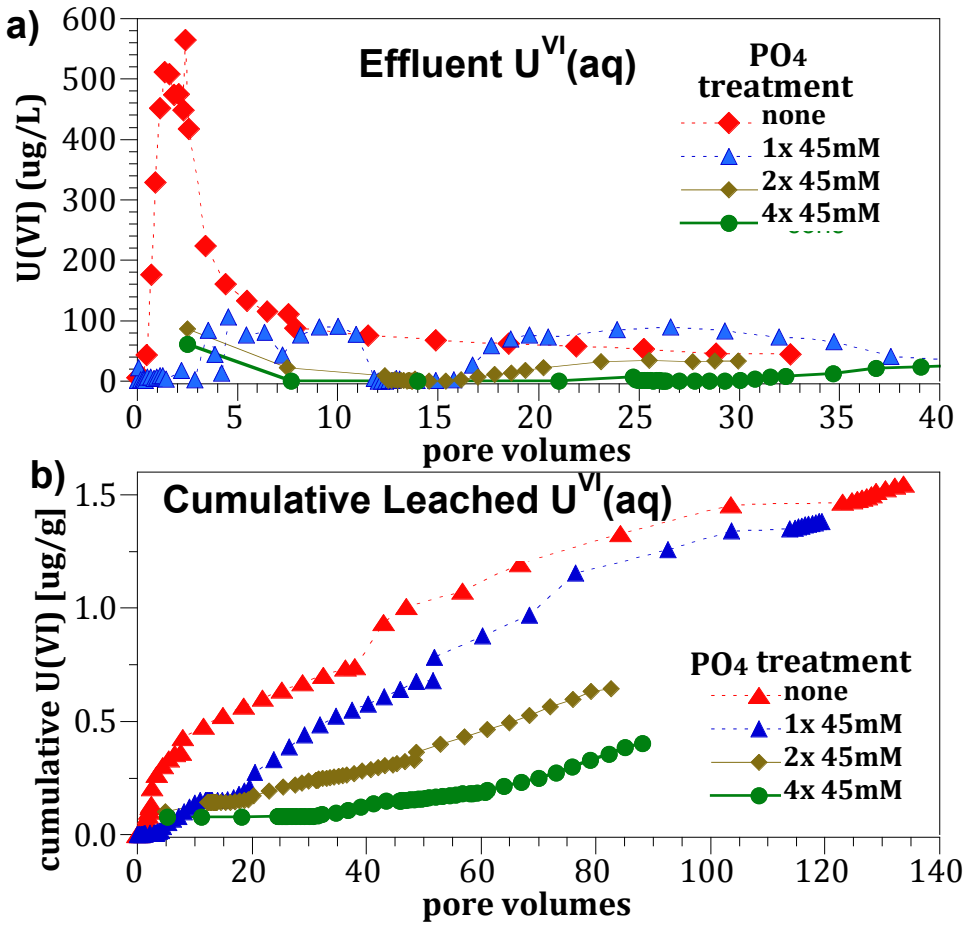

Figure 6. Comparison of Uranium Leaching Results for Columns Conducted with 32.1 μg/L Uranium Influent Concentration: a) Effluent U(VI) Concentration, and b) Cumulative Leached Mass.

4.3 Changes in Uranium Surface Phases

Uranium extractions were conducted on untreated/unleached sediment, untreated/leached, and PO_4-treated/leached sediments (Figure 7). A total of 18 extractions were done, with 6 for the untreated and duplicates for leached sediments. The variability in the extractions shown in Figure 7a for six untreated samples is (reported as standard deviation, Table B1) ± 3.0% for aqueous U, ± 0.7% for adsorbed U, ±1.7% for rind carbonate U (acetate pH 5), ± 2.7% for all carbonate U (acetate pH 2.3), ±1.6% for oxide U (oxalic acid), and ± 6.5% for remaining hard to extract U phases (8M HNO3). The untreated/unleached extractions showed 7.4% of the uranium was aqueous and adsorbed, 56.3% was carbonate associated, and

36.2% was in oxide, sulfide, silicate, and other hard to extract phases (Table 5). The total uranium extracted in the sediment averaged 1.39 ± 0.11 μg/g.

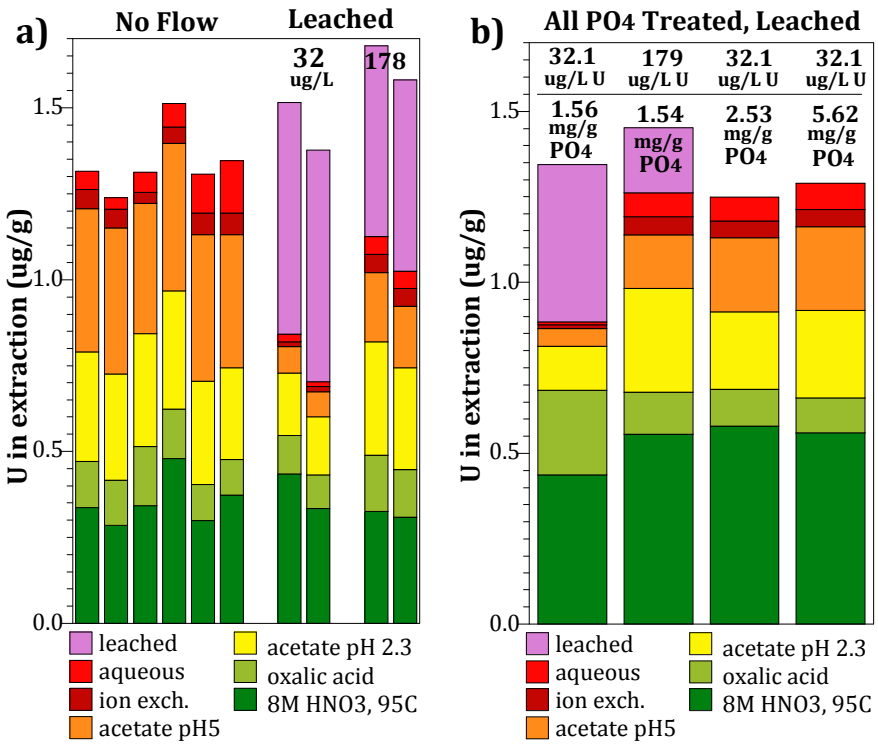

Figure 7. Uranium Extractions for: a) untreated sediments, and b) PO_4-treated sediments. Leached represents net leached from sediment (effluent – influent).

Table 5. Uranium Extraction Summary

#	PO4 treatment	U(VI) aq. +ads. (ug/g)	U(VI) carbonate (ug/g)	U(VI) hard to extr. (ug/g)	U(VI) total (ug/g)	U(VI) net leached (ug/g)
no flow	none	0.096	0.726	0.467	1.388 ± 0.109	--
post C55	none	0.103	0.505	0.467	1.075 ± 0.071	0.735
post C56	1 x 45 mM	0.122	0.460	0.679	1.260 ± 0.482	0.220
post C54	none	0.032	0.251	0.489	0.772 ± 0.0981	0.893
post C57	1 x 45 mM	0.020	0.180	0.684	0.884 ± 0.250	0.536
post C58	2 x 45 mM	0.119	0.442	0.687	1.248 ± 0.426	-0.002
post C59	4 x 45 mM	0.128	0.499	0.662	1.289 ± 0.0116	-0.337

Leaching the untreated sediment resulted in mobilization of 52.9% (experiment C55) or 64.2% (experiment C54) of the uranium from the sediment. Post-leach extractions have about the same concentration of aqueous and adsorbed U (since U is continuously flowing into columns), but less carbonate-associated uranium (Figure 7a), and the same oxide, sulfide, silicate, and other hard to extract uranium phases (which are less mobile).

Leaching the phosphate-treated sediments (Figure 7b) dramatically decreased the net uranium leaching (which was directly proportional to the phosphate precipitate concentration, Section 4.4), as shown by

smaller purple extractions in Figure 7b with higher phosphate concentrations, and in Table 5, last column. The phosphate treatment resulted in an increase in the in the oxide and hard to extract uranium phases (0.49 to 0.69 μg/g) compared to untreated sediment (0.47 μg/g).

Given the low uranium concentration in the sediment (1.4 μg U/g sediment), changes in uranium surface phases could not be identified by x-ray diffraction (the minimum limit is about 0.5% or 5000 μg/g). The use of an electron microprobe, which can identify element associations (and infer crystal structure) on a micron scale, is also unlikely to be effective, given a detection limit of 50 to 100 μg/g. Specific experiments would need to be conducted that contain higher uranium concentrations in the sediment in order to be able to identify change in uranium surface phases, as was described earlier in previous studies in Section 2.2. In one phosphate-treated sediment experiment (C59, Table 5), four phosphate treatments were conducted on the uranium-contaminated Old Rifle sediment in which effluent samples for each treatment (about 200 mL) were collected in a single vial rather than multiple vials. In the vial for the first phosphate treatment, over the course of a week, precipitate formed, which was analyzed and dried. This precipitate was identified by x-ray diffraction as brushite (a hydrous Ca-phosphate, $CaHPO_4 \bullet 2H_2O$, Figure 8). Subsequent washing of the precipitate with an ion exchange solution (0.5 mol/L $MgNO_3$) did not wash off any uranium, but dissolution of the precipitate in 0.5 mol/L HNO_3 acid indicated the precipitate contained 460 μg uranium per gram of precipitate. This is equivalent to 0.05% U, so clearly could not be identified with x-ray diffraction, but may be identifiable using an electron microprobe. It is likely that this hydrous Ca-phosphate precipitate will crystallize into apatite over time. It is not known whether the brushite precipitate is representative of uranium precipitation that actually occurred within the sediment column.

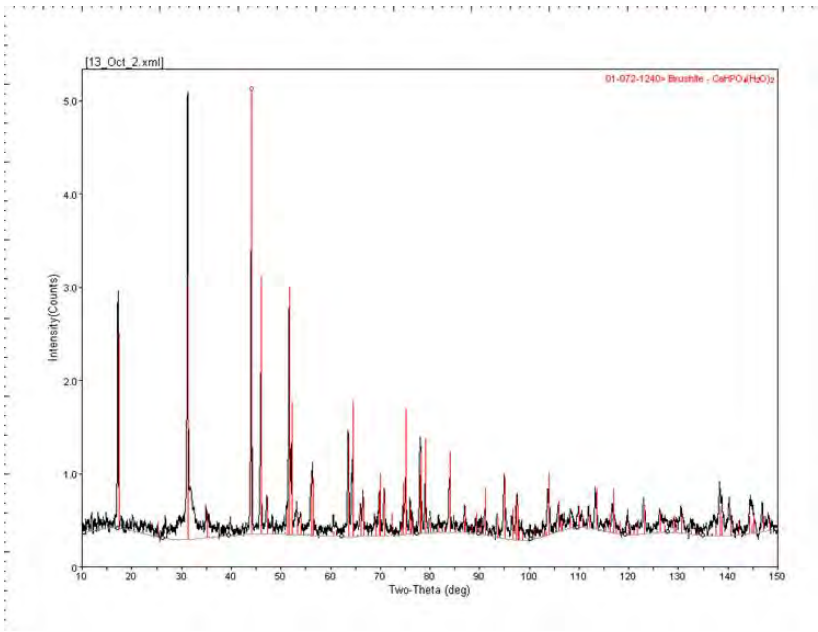

Figure 8. X-Ray Diffraction Results of Precipitate in an Effluent Sample from a Phosphate-Treated Sediment (Experiment C59) in Black with Pattern of Brushite ($CaHPO_4 \bullet 2H_2O$) in Red.

4.4 Phosphate Precipitation Loading in the Sediment

The mass of phosphate in the sediment columns was calculated from the phosphate injected minus the phosphate in effluent samples (Table 6). For sediment columns that received a single 45 mM phosphate treatment for 12 pore volumes, the average mass of phosphate was 1.54 to 1.56 mg/g. With two

phosphate injections separated by a stop-flow phase, the mass of phosphate was almost twice (2.86 mg/g), and four injections about 4 times greater (5.96 mg/g).

Table 6. Phosphate Loading in Sediment Columns

#	injection U conc. (ug/L)	number of PO_4 injections	PO_4 injected (mmol)	PO_4 effluent (mmol)	PO_4 in sed. (mg/g)
C57	32.1	1	17.336	15.764	1.558
C56	383	1	14.107	12.588	1.541
C58	32.1	2	15.858	12.751	2.865
C59	32.1	4	31.793	25.878	5.956

4.5 Uranium Leaching and Uptake Rate in Untreated and PO_4-Treated Sediments

As described qualitatively in previous sections, some uranium(VI) from surface phases (i.e., adsorbed and/or carbonate associated or other phases) is slowly partitioning from the surface into the aqueous solution during leaching experiments. This effect is most clearly observed for untreated sediments. For phosphate-treated sediments, a range of uranium leaching behavior was observed from less uranium leaching compared to untreated sediment (for low phosphate treatments) to actually no uranium leaching and influent uranium uptake (for high phosphate treatments). The rate of uranium release from the sediment (or net uptake) was calculated during continuous flow and also during stop-flow events. For continuous flow, the effluent minus influent uranium concentration represents the amount of uranium released (or uptaken) divided by the average residence time in the column at a specific flow rate (Table 7). For stop-flow events, the increase in uranium during the stop flow divided by the stop-flow time represents the uranium release rate (Table 8).

For the continuous flow data (Table 7), there are multiple U(VI) release rates calculated for each experiment because there are two to three different flow rates in each experiment. Untreated sediment generally had high positive values (i.e., net release of uranium from the sediment) whereas higher and higher phosphate treatments had high negative values (i.e., net uptake of uranium by the sediment). These results are presented in graphical form correlated with phosphate mass in Section 5.3.

Table 7. Uranium Release Rates During Continuous Flow

#	PO4 treatment	U(VI) inject conc. (ug/L)	Flow Rate (ft/day)	U(VI) effluent (ug/L)	U(VI) rel. rate* (ug/Kg/day)
C55	none	178.85	4.27	213.5	63.7
		383.4	0.383	380.2	-0.56
C56	1 x 45 mM	178.85	2.84	214.7	2.20
		383.4	0.258	349.2	-5.71
C54	none	32.1	4.19	38.51	14.6
		32.1	0.371	43.49	2.25
C57	1 x 45 mM	32.1	3.46	44.85	14.1
		32.1	0.283	17.42	-4.85
C58	2 x 45 mM	32.1	2.68	33.1	-16.7
		32.1	0.822	21.21	-9.85
		32.1	0.32	4.97	-4.43
C59	4 x 45 mM	32.1	2.71	21.85	-36.5
		32.1	0.813	11.1	-13.9
		32.1	0.298	8.93	-3.77

* + is U release from sed., - is U uptake by sed.

Table 8. Uranium Release Rates During Stop-Flow Events

#	PO4 treatment	stop (pore vol)	U(VI) stop conc. (ug/L)	U(VI) start conc. (ug/L)	U(VI) rel. rate* (ug/Kg/day)
C55	none	2.0	450.5	371.2	-8.60
		39.6	204.1	259.4	1.01
C56	1 x 45 mM	14.6	0.74	1.33	0.30
		44.2	196.3	120.3	-3.99
C54	none	2.4	448.2	564.6	13.3
		38.0	44.40	188.6	2.80
C57	1 x 45 mM	14.6	4.59	3.73	-0.416
		44.2	50.44	53.9	0.174
C58	2 x 45 mM	13.8	0.48	3.20	1.39
		29.9	33.36	34.5	0.065
		44.6	33.21	9.54	-0.513
C59	4 x 45 mM	11.5	0.33	0.55	0.109
		43.5	30.70	8.51	-1.228
		58.00	14.71	2.95	-0.246

* + is U release from sed., - is U uptake by sed.

For stop-flow data (Table 8), the same correlation occurs, with (generally) positive values for untreated sediment (uranium release by the sediment) and negative values for phosphate-treated sediments, although there is more variability compared with continuous flow data.

4.6 Uranium Sorption

Uranium sorbs to the Old Rifle sediment in untreated and phosphate-treated sediments. Uranium sorption in untreated and post leached sediment was measured from: a) aqueous and adsorbed uranium extractions in Section 4.3, and b) breakthrough data after stop-flow events in columns (Table 9). The K_d values were all relatively small (below 2.3) in the high carbonate Old Rifle groundwater, as expected. The uranium sorption onto the apatite or phosphate precipitate by itself has not been measured in the Old Rifle groundwater, but there appeared to be no correlation between the phosphate loading and the resulting K_d (Table 9 and Figure 9). The hypothesis that uranium is sorbing to apatite is not supported by: a) the lack of change of K_d values in PO_4-treated sediments (Table 9), and b) the lack of change in adsorbed uranium in post leach extractions for PO_4-treated sediments (dark red extraction, Figure 7b). Therefore, these conclusions along with change in uranium uptake rate with PO_4 loading (Section 5.2) support the hypothesis that a U-PO_4 precipitate (such as autunite) is forming.

Table 9. Uranium Release Rates During Stop-Flow Events

#	PO4 treatment	U(VI) inject conc. (ug/L)	breakthrough data U(VI) Rf	breakthrough data U(VI) K_d (cm^3/g)	extractions U(VI) K_d (cm^3/g)
no flow					1.080
C55	none	179, 383	6.80	1.33	0.522
C56	1 x 45 mM	179, 383	4.16	0.68	0.891
C54	none	32.1	7.10	1.94	0.518
C57	1 x 45 mM	32.1	5.82, 2.70	1.48, 0.52	0.513
C58	2 x 45 mM	32.1	6.92, 7.20	1.45, 1.52	0.968
C59	4 x 45 mM	32.1	10.9, 7.50	2.35, 1.54	0.704

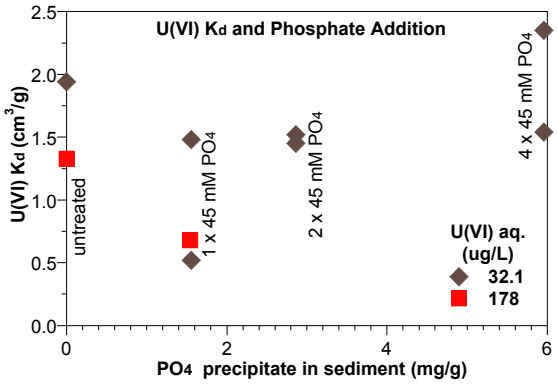

Figure 9. Uranium Sorption Based on U(VI) Breakthrough Data and Phosphate Loading.

5.0 Discussion

5.1 PO_4 Treatment and Source Area Stabilization: Sediment Uranium Mobility

The six leaching experiments for untreated and PO_4-treated Old Rifle sediments showed uranium in the effluent that was from both the sediment (i.e., desorbed/dissolved U surface phases) and from influent uranium that was not retained by the sediment. Leaching experiments with no uranium in the influent would also not be representative of Old Rifle field conditions. A plot of cumulative effluent uranium minus influent uranium (Figure 10) effectively separates uranium leaching from the sediment (i.e., for source area treatment) from retention of influent uranium (i.e., permeable reactive barrier application). Plots of effluent uranium and uranium influent (Figures 4b, 4d, 5b, 5d, 6b) which have effluent greater than influent clearly show uranium is leaching from the sediment, but with high phosphate treatment, and effluent uranium less than influent uranium (Figure 4d), no uranium is leaching from the sediment and some influent uranium is also removed from solution. For the plot of effluent minus influent cumulative uranium (Figure 10, a positive value represents uranium leaching off the sediment, a value of zero represents no leaching from the sediment, and a negative value represents net uptake of uranium by the sediment (i.e., some uranium influent is removed from aqueous solution).

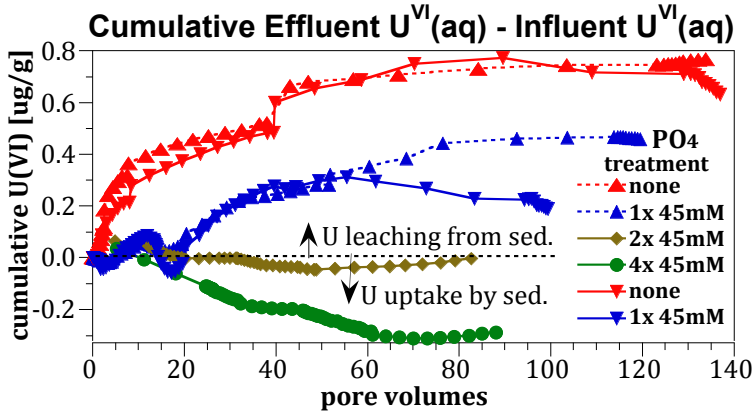

Figure 10. Uranium Cumulative Effluent Minus Influent in Leaching Experiments for Untreated and PO_4-Treated Old Rifle Sediments.

The cumulative effluent minus influent uranium for untreated sediments (red triangles, Figure 10) show a large increase initially (from the initial high concentration uranium), then continued leaching of a total of 0.7 μg/g U, or about 50% of the total uranium in the sediment (1.39 ± 0.11 μg/g, Table 5 and Figure 6). The post-leach uranium extractions (Figure 7) show that most of this leached uranium was carbonate associated, as aqueous/adsorbed uranium is still in equilibrium with the sediment (because uranium is still present in the influent). For phosphate-treated sediments, the cumulative effluent minus influent uranium decreased with increasing phosphate treatment. For minimal phosphate treatment (i.e., a single 45 mM PO_4 injection), the net uranium effluent was 0.2 to 0.4 μg/g (compared to 0.7 μg/g for untreated), indicating effective source area treatment. For moderate phosphate treatment (i.e., two 45 mM PO_4 injections), the net uranium effluent was 0.0 μg/g, indicating on average, all uranium in the sediment was immobilized (but can also represent some uranium in the sediment was mobilized and the same mass of uranium in the influent was removed by phosphate in the sediment). For high phosphate treatment (i.e., four 45 mM PO_4 injections), there was a net -0.33 μg/g of uranium leached from the sediment (meaning 0.33 μg/g in the influent was removed by the phosphate in the sediment. The high phosphate treatment represents a case where (on average) all uranium in the sediment was immobilized (i.e., effective source area treatment) and the phosphate-laden sediment is also acting as a permeable reactive barrier (details discussed further in the following section). As described in Section 5.3 (phosphate loading versus effectiveness), about 2 mg of phosphate per gram of sediment are needed for effective source area treatment, but greater phosphate mass is required for effective use as a permeable reactive barrier.

Although the mechanism by which the phosphate treatment is removing uranium has not been positively identified, it is not sorption (Section 4.6), which can only retard uranium movement < 8 pore volumes (Table 9, Figure 9) and did not change with higher PO_4 loading (nor did the fraction adsorbed uranium change in PO4-treated sediments, Figure 7b, dark red extraction). Based on previous studies, uranium is either precipitated in low solubility phosphate phase such as autunite or coated and immobilized by the phosphate precipitate (i.e., hydroxyapatite). While coating by non-uranium-bearing phosphate precipitates can occur, it could not explain the active uptake of uranium by the phosphate-laden sediment that is observed (see following section). This uptake is consistent but not definitive proof of the formation of a uranium-phosphate phase.

5.2 PO_4 Treatment for Permeable Reactive Barrier: Aqueous Uranium Mobility

Sufficiently high phosphate treatment of Old Rifle sediments results in significantly reduced leaching of uranium by: a) immobilization of nearly all uranium in the sediment (source area treatment), and b) removal of significant amounts influent uranium from solution (i.e., permeable reactive barrier application), as described in the previous section. The effectiveness of the phosphate treatment as a permeable reactive barrier is better at average Old Rifle groundwater velocities (Figure 11a, 0.28 ft/day), but decreases in effectiveness at 3 times that average Old Rifle groundwater velocity (Figure 11b) or 10 times the average Old Rifle groundwater velocity (Figure 11c). This is a result of the relatively *slow* uptake of uranium by phosphate precipitates. In other words, rapid flow rates have uranium flux rates that are than the phosphate uptake rate. For experiments conducted at high (178, 383 μg/L) uranium influent concentration, effectiveness of the phosphate treatment was also low. This is because the high uranium concentration (even at low velocity) exceeded the ability of the phosphate treatment (at 1.5, 2.9 or 5.96 mg/g loading) to uptake uranium (plots in Appendix C) at this uranium flux rate. A plot of uranium uptake (or release) rates as a function of the groundwater velocity (Figure 12) shows efficient uptake of uranium by the phosphate-laden sediment at low velocities, but less effectiveness at higher velocities. A summary table of the effectiveness of the phosphate treatment for use as a permeable reactive barrier (blue section, Table 10) shows the fraction of uranium in the influent that is removed from aqueous

solution increases with greater phosphate treatment. At the highest phosphate treatment used in this study (experiment C59, 5.96 mg/g) even at low velocity and low uranium concentration (32.1 µg/L), a maximum of 77% of the uranium is removed (i.e., and 23% advects down gradient). However, greater effectiveness as a permeable reactive barrier could be achieved with a wider phosphate treatment barrier (i.e., to allow a higher uptake rate relative to the influent uranium flux) or possibly higher phosphate loading.

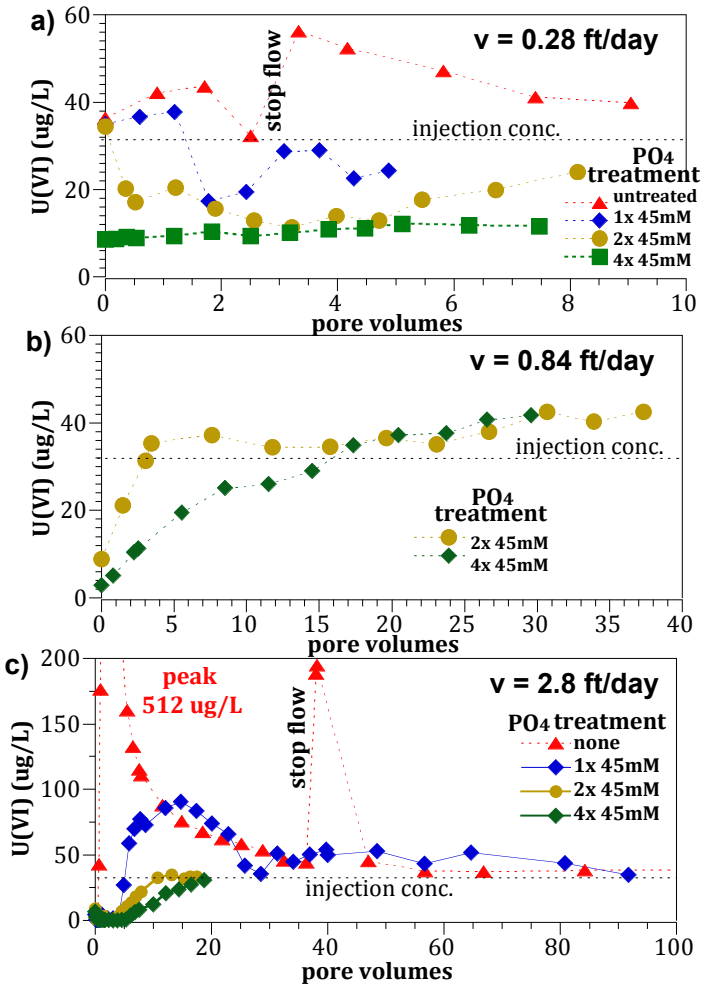

Figure 11. Uranium Effluent Concentrations with 32.1 µg/L Influent and Velocity of a) 0.28 ft/day, b) 0.84 ft/day, and c) 2.8 ft/day.

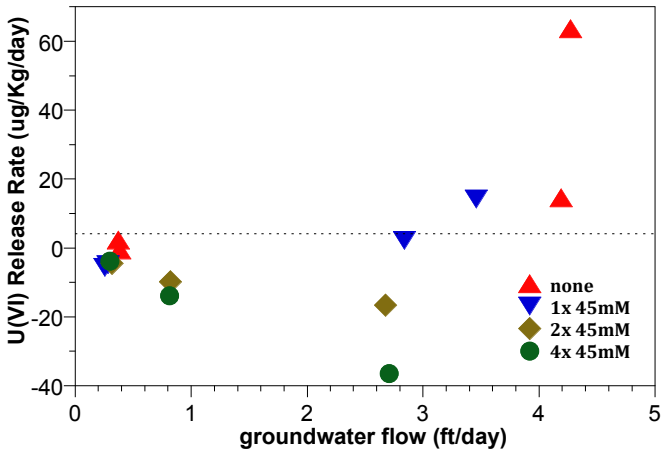

Figure 12. Uranium Release or Uptake Rate as a Function of Groundwater Velocity. Rates calculated from continuous flow data.

Table 10. Phosphate Treatment Effectiveness

		injection		for permeable reactive barrier			for source area treatment		
#	treatment	U conc. (ug/L)	sed. PO_4 (mg/g)	vel.* (ft/day)	effluent U (ug/L)	% immobilized	maximum pore vol.	mobilized sed. U (ug/g)	% immobilized
C54	none	32.1	--	0.37	43.5	--	134	0.675	--
C57	1x Ca-cit-PO_4	32.1	1.56	0.28	20.8	52.2	120	0.399	40.9
C58	2x Ca-cit-PO_4	32.1	2.86	0.32	16.9	61.1	85	< 0.01	100
C59	4x Ca-cit-PO_4	32.1	5.96	0.30	10.1	76.8	92	< 0.01	100
C55	none	178, 383	--	0.38	361	--	137	0.554	--
C56	1x Ca-cit-PO_4	178, 383	1.56	0.26	318 - 384	0.0 - 12.1	99.4	0.166	70.0

* low (average Rifle) velocity

5.3 Phosphate Loading Effect on Uranium Uptake Mass and Rate

As shown in previous sections, while any phosphate treatment reduced the uranium leaching from the sediment (i.e., source area application), greater amounts of phosphate treatment were needed to have some influence on the uranium flowing into the sediment column (i.e., permeable reactive barrier application). All of the experimental data shows that there is net uranium uptake from influent at a phosphate loading of 2.9 mg PO_4/g or greater (Figure 13b) and that the uranium uptake rate is higher for greater mass of phosphate (Figure 13a). A plot of the uranium release (or uptake) rate as a function of the amount of phosphate in the sediment (Figure 13a, based on continuous flow data) shows active uptake rates at higher phosphate loadings, as well as the effects of velocity and the uranium injection concentration. With no phosphate treatment, uranium release rates were highest with high uranium injection concentration, and were all positive (i.e., uranium released from the sediment). Phosphate treatment at all velocities resulted in uranium uptake (i.e., negative uranium release rates). Experiments with low uranium injection concentration (32.1 μg/L) at high velocity (3.4 ft/day) conducted at three phosphate loadings (purple triangles, Figure13a) and showed a consistent trend of increasing uranium uptake by the sediment. Interestingly, at the highest phosphate treatment, lower velocities appeared to have slower uranium uptake rates (i.e., orange and black diamonds, (Figure 13a), although at low

velocities, the change in uranium concentration was smaller, so smaller rates were calculated. Again, the same trend of greater uranium uptake with increasing phosphate loading was observed.

It is clear that in order for phosphate treatment to be effective as a permeable reactive barrier, high phosphate loadings are needed (6 mg PO_4/g of sediment or higher) because permeable reactive barriers are evaluated on the basis of concentration in the effluent side versus influent (Table 10). Based on these results, 77% immobilization of influent uranium for the 5.96 mg PO_4/g loading (experiment C59, Table 10) can be expected. The uranium influent flux in this experiment is based on natural Old Rifle groundwater velocity (0.3 ft/day) at a concentration of 32.1 μg/L.

For source area treatment, while any phosphate loading decreased the mass of uranium leading from the sediment, the loading of 2.9 mg PO_4/g sediment (or higher, 10) resulted in all of the uranium in the sediment being immobilized for at least 90 pore volumes. The longevity of the treatment is likely much greater, as either low solubility U-phosphate precipitates are created and/or non-uranium Ca-phosphate precipitates are coating uranium surface phases (all of which are low solubility). Previous studies at low phosphate loading have for 500 pore volumes have demonstrated the potential for longevity of the phosphate treatment (Appendix F).

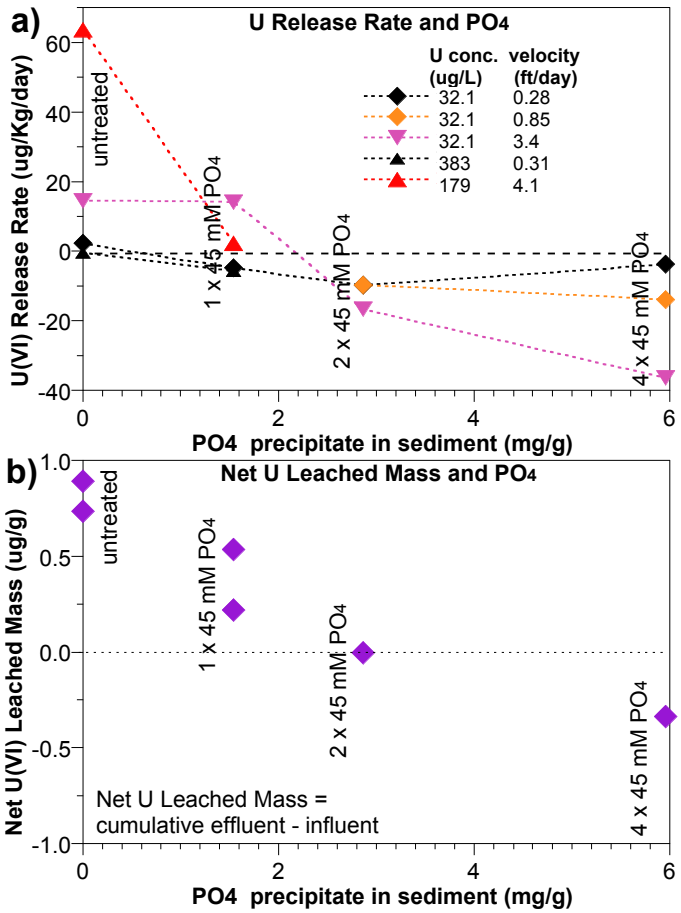

Figure 13. Phosphate Treatment Effect on a) Uranium Release or Uptake Rate, and b) Net Leached U Mass.

6.0 Summary and Recommendations

The purpose of this study was to conduct laboratory scale proof of principle experiments to evaluate the effectiveness of a hydroxyapatite [$Ca_{10}(PO_4)_6(OH)_2$] permeable reactive barrier and source area treatment to decrease uranium mobility at the DOE former Old Rifle uranium mill site. The effectiveness of phosphate treatment impact was evaluated by comparing uranium leaching and surface phases in untreated and PO_4-treated sediments. These results show both changes in uranium leaching from the sediment (i.e., source area treatment application), and changes in uranium uptake by the PO_4-laden sediment (i.e., permeable reactive barrier application). The impact of the amount of phosphate precipitation in the sediment on uranium mobility was evaluated with three different phosphate loadings. A range of flow velocity and uranium concentration conditions (i.e., uranium flux through the phosphate-treated sediment) was also evaluated to quantify the uranium uptake mass and rate by the phosphate precipitate.

Phosphate treatment decreased the mass and rate of uranium leached from the sediment in direct proportion to the amount of phosphate precipitated. Low phosphate treatment decreased uranium leached mass from the sediment by 40 to 70% and had little effect on the aqueous uranium flowing through the PO_4 treated sediment, whereas high phosphate treatment decreased uranium leached mass from the sediment by 100% and removed at much as 77% of aqueous uranium flowing through the PO_4 treated sediment. More specifically, for source area application, at a phosphate loading of 3 mg PO_4/g of sediment or more, uranium surface phases were not released during 90 pore volumes of groundwater injection. For permeable reactive barrier application, a higher phosphate loading of 6 mg PO_4/g of sediment (highest phosphate loading tested) was needed to achieve continuous removal of 77% of the aqueous uranium flowing into the PO_4-treated sediment. The rate of uranium removal by phosphate precipitate ranged from 5 to 35 μg U/Kg sediment/day, so the PO_4-treated sediment was effective at low aqueous uranium concentration (32.1 μg/L) at natural Old Rifle groundwater flow rates (0.3 ft/day), but was less effective at higher uranium flux rates (higher uranium concentration or more rapid flow rates). Characterization of the multiple uranium surface phases showed that the untreated/unleached sediment contained 1.39 ± 0.11 μg U/g of sediment with 7.4% of the uranium aqueous and adsorbed, 56.3% carbonate associated, and 36.2% was in oxide, sulfide, silicate, and other hard to extract phases.

Leaching the untreated sediments mobilized 53 to 64% of the uranium, which was mainly carbonate-associated uranium along with adsorbed uranium. Uranium in oxides, sulfides, silicates and other hard to extract phases were not mobilized. The phosphate treatment resulted in an increase in the in the oxide and hard to extract uranium phases (0.49 to 0.69 μg/g) as compared to the untreated sediment (0.47 μg/g), accounting for the dramatic decrease in leaching. Aqueous and adsorbed uranium were unchanged because aqueous uranium was continuously injected in the inlet to maintain sorption equilibrium (and approximate Old Rifle Site conditions). During phosphate treatment of the sediment, a precipitate that formed in the effluent was identified by x-ray diffraction as brushite (a hydrous Ca-phosphate, $CaHPO_4 \cdot 2H_2O$). This phosphate phase is likely to crystallize into apatite over time. Subsequent treatment of the brushite precipitate with an ion exchange solution did not desorb uranium, but acid dissolution of the precipitate indicated it contained 460 μg U/g. Although the mechanism by which the phosphate treatment is removing uranium has not been positively identified, evidence points toward formation of a U-PO_4 precipitate including: a) increase in U uptake rate with higher PO_4 concentration (Figure 13a), b) lack of change in adsorbed uranium in post leach extractions for PO_4-treated sediments (dark red extraction, Figure 7b), c) lack of change of K_d values in PO_4-treated sediments (Table 9), and d) uptake of aqueous uranium from influent water (Figure 13b, highest PO_4 loading). Although identification of the U surface phase(s) in the PO_4-treated sediments was not conducted in this study, it is likely to yield inconclusive results due to the low uranium concentration in the sediment (1.4 μg U/g). In addition, while coating by non-uranium-phosphate precipitates can occur and could explain lower leaching of

uranium from the sediment, it cannot explain the uptake of aqueous uranium in the influent water by the phosphate-laden sediment (Figure 13b). These multiple lines of evidence are consistent with (but do not prove) the formation of a U-PO_4 precipitate (such as autunite) hypothesis and not sorption or coating by a non-uranium phosphate precipitate exerts significant control in reducing uranium leaching from both sediment and aqueous solution.

Overall, these results demonstrate that sufficient phosphate treatment of the sediment can be a viable remediation strategy for source area treatment of uranium, and under higher phosphate loading and/or low uranium flux, as a permeable reactive barrier. Additional laboratory scale experiments could further optimize the phosphate treatment and provide information to measure or predict the longevity. These experiments include: a) identification of uranium surface phases (to predict longevity); b) quantification of the optimal PO_4 mass needed for PRB application; c) quantification of U sorption to apatite, d) quantification of Ca-citrate-PO_4 treatment under varied redox conditions (present at the Rifle Site); and e) measurement of the long-term performance of the PO_4-treated sediments (ended at 90-140 pore volumes) at 500 to 1000 pore volumes.

7.0 References Cited

Andronescu E, E Stefan, E Dinu, and C Ghitulica. 2002. “Hydroxyapatite Synthesis.” Key Engineering Materials 206-213:1595-1598.

Bailey JE and DF Ollis. 1986. Biochemical Engineering Fundamentals. McGraw-Hill Publishing Co., New York.

Bond D, J Davis, and JM Zachara. 2008. “Uranium(VI) Release from Contaminated Vadose Zone Sediments: Estimation of Potential Contributions from Dissolution and Desorption.” In Adsorption of Metals to Geomedia II, MO Barnett and DB Kent (eds.), U.S. Geological Survey, Menlo Park, California, and Pacific Northwest National Laboratory, Richland, Washington.

Brina R and AG Miller. 1992. “Direct Detection of Trace Levels of Uranium by Laser-Induced Kinetic Phosphorimetry.” Analytical Chemistry 64(13):1413–1418.

Bynhildsen L and T Rosswall. 1997. “Effects of Metals on the Microbial Mineralization of Organic Acids.” Water, Air, and Soil Pollution 94(1-2):45-57.

Campbell, K.M, R.K Kukkadapu, N.P. Qafoku, A.D. Peacock, E. Lesher, K.H. Williams, J.

Bargar, M.J. Wilkins, L. Figueroa, J. Ranville, J.A. Davis and P.E. Long, 2012. "Geochemical, Mineralogical and Microbiological Characteristics of Sediment from a naturally Reduced Zone in a Uranium-Contaminated Aquifier" Applied Geochemistry 27 2012 pp. 1499-1511

Catalano J, J McKinley, J Zachara, S Heald, S Smith, and G Brown. 2008. “Changes in Uranium Speciation Through a Depth Sequence of Contaminated Hanford Sediments.” Environmental Science and Technology 40(8):2517–2524.

Chao TT and L Zhou. 1983. “Extraction Techniques for Selective Dissolution of Amorphous Iron Oxides from Soils and Sediments.” Soil Science Society of America Journal 47:225–232.

Elliot JC, PE Mackie, and RA Young. 1973. “Monoclinic Hydroxyapatite.” Science, 180:1055-1057.

Hyun, S. P., P. M. Fox, J. A. Davis, K.M. Campbell, K. F. Hayes, and P. E. Long, 2009. "Surface Complexation Modeling of U(VI) Adsorption by Aquifer Sediments from a Former Mill Tailings Site at Rifle, Colorado", Environmental Science and Technology, 43(24), pp.9368-9373.

Kohler M. DP Curtis, DE Meece, and JA Davis. 2004. "Methods for Estimating Adsorbed Uranium (VI) and Distribution Coefficients of Contaminated Sediments." Environmental Science and Technology 38:240–247.

Komlos, J., A. Peacock, R. K. Kukkadapu, and P. R. Jaffe, 2009. "Long term Dynamics of Uranium Reduction/Reoxidation Under Low Sulfate Conditions" Geochimica Cosmochimca Acta, 72(15), 3603-3615.

Liu C, J Zachara, N Qafoku, and Z Wang. 2008. "Scale-Dependent Desorption of Uranium from Contaminated Subsurface Sediments." Water Resources Research 44:2454–2461.

Misra DN. 1998. "Interaction of Some Alkali Metal Citrates with Hydroxyapatite - Ion-Exchange Adsorption and Role of Charge Balance." Colloids and Surfaces a-Physicochemical and Engineering Aspects 141:173-179.

Moore RC, C Sanchez, K Holt, P Zhang, H Xu, and GR Choppin. 2004. "Formation of Hydroxyapatite in Soils Using Calcium Citrate and Sodium Phosphate for Control of Strontium Migration." Radiochimica Acta 92(9-11/2004):719-723.

Moore R, J Szecsody, M Truex, K Kelean, R Bontchev, and C Ainsworth. 2007. "Formation of Nanosize Apatite Crystals in Sediments for Contaminant and Stabilization of Contaminants." Environmental Applications of Nanomaterials, Synthesis, Sorbents, and Sensors, (eds) G Fryxell and G Cao, Imperial College Press, p. 89-109.

Moore, RC and MJ Rigali, 2015 "Preliminary Assessment of an Apatite Reactive Barrier for the DOD Old Rifle Site" SAND2015-8403. Sandia National Laboratories, Albuquerque New Mexico.

Papargyris AD, AT Botis, and SA Papargyri. 2002. "Synthetic Routs for Hydroxyapatite Powder Production." Key Engineering Materials 206-213:83-86.

Shi Z, C Liu, J Zachara, Z Wang, and B Deng. 2009. "Inhibition Effect of Secondary Phosphate Mineral Precipitation on Uranium Release from Contaminated Sediments." Environmental Science and Technology 43:8344–8349.

Smith SC and J Szecsody. 2011. "Influence of Contact Time on the Extraction of 233-Uranyl Spike and Contaminant Uranium from Hanford Site Sediment." Radiochimica Acta 99:693–704.

Sumner ME. 2000. "Soil Fertility and Plant Nutrition." Section D in Handbook of Soil Science, CRC Press, Boca Raton, Florida.

Szecsody, J.E., M. J. Truex, L. Zhong, T.C. Johnson, N.P. Qafoku, M.D. Williams, J.W. Greenwood, E.L. Wallin, J.D. Bargar, and D.K. Faurie, 2012a. Geochemical and Geophysical Changes During NH_3 Gas Treatment of Vadose Zone Sediments for Uranium Remediation, Vadose Zone Journal, 11(4).

Szecsody, J., L. Zhong, M. Oostrom, V. Vermeul, J. Fruchter, M. Williams, 2012b, Use of polyphosphate to decrease uranium leaching in Hanford 300 area smear zone sediment. Pacific Northwest National Laboratories PNNL-21733

Szecsody J, M Rockhold, M Oostrom, R Moore, C Burns, M Williams, L Zhong, J Fruchter, J McKinley, V Vermeul, M Covert, T Wietsma, A Breshears, and B Garcia. 2009. Sequestration of Sr-90 Subsurface Contamination in the Hanford 100-N Area by Surface Infiltration of a Ca-Citrate-Phosphate Solution. PNNL-18303, Pacific Northwest National Laboratory, Richland, Washington.

US DOE, 1999. "Final Site Observational Work Plan for the UMTRA Project Old Rifle Site."

Document number U0042501, GJO-99-88-TAR Rev. 1.

US DOE, 2012. "Groundwater Compliance Action Plan for the Old Rifle, Colorado UMTRCA Title I Processing Site" LMS/RFO/507857.

Van der Houwen JAM and AE Valsami-Jones. 2001. "The Application of Calcium Phosphate Precipitation Chemistry to Phosphorus Recovery: The Influence of Organic Ligands." Environmental Technology 22:1325-1335.

Vermeul VR, BN Bjornstad, BG Fritz, JS Fruchter, RD Mackley, DR Newcomer, DP Mendoza, ML Rockhold, DM Wellman, and MD Williams. 2009. 300 Area Uranium Stabilization Through Polyphosphate Injection: Final Report. PNNL-18529, Pacific Northwest National Laboratory, Richland, Washington.

Wellman DM, JS Fruchter, VR Vermeul, E Richards, DP Jansik, and E Edge. 2011. "Evaluation of the Efficacy of Polyphosphate Remediation Technology: Direct and Indirect Remediation of Uranium Under Alkaline Conditions." Technology and Innovation 13:151–164.

Wellman DM, EM Pierce, DH Bacon, M Oostrom, KM Gunderson, SM Webb, CC Bovaird, EA Cordova, ET Clayton, KE Parker, RM Ermi, SR Baum, VR Vermeul, and JS Fruchter. 2008a. 300 Area Treatability Test: Laboratory Development of Polyphosphate Remediation Technology for in Situ Treatment of Uranium Contamination in the Vadose Zone and Capillary Fringe. PNNL-17818, Pacific Northwest National Laboratory, Richland, Washington.

Wellman DM, JN Glovack, K Parker, EL Richards, and EM Pierce. 2008b. "Sequestration and Retention of Uranium(VI) in the Presence of Hydroxylapatite under Dynamic Geochemical Conditions." Environmental Chemistry 5(1):40–50.

Zachara J, C Liu, C Brown, S Kelly, J Christensen, J McKinley, J Davis, J Serne, E Dresel, and W Um. 2007. A Site-Wide Perspective on Uranium Geochemistry at the Hanford Site. PNNL-17031, Pacific Northwest National Laboratory, Richland, Washington.

Zhong, L. J.E. Szecsody, M.J. Truex, M.D. Williams, Y. Liu. 2015. Ammonia Gas Interaction with Sediments and Pore Water and Induced Uranium Immobilization under Vadose Zone Conditions. J. Haz. Materials. 289:118–129. http://dx.doi.org/10.1016/j.jhazmat.2015.02.025

Appendix A

1-D Column Individual Experiment Results

Appendix A
1-D Column Individual Experiment Results

Column Experiment C54

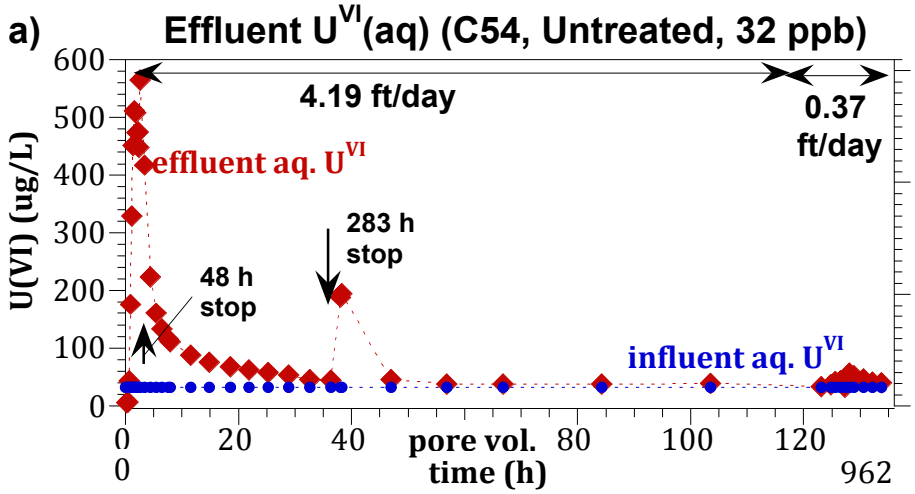

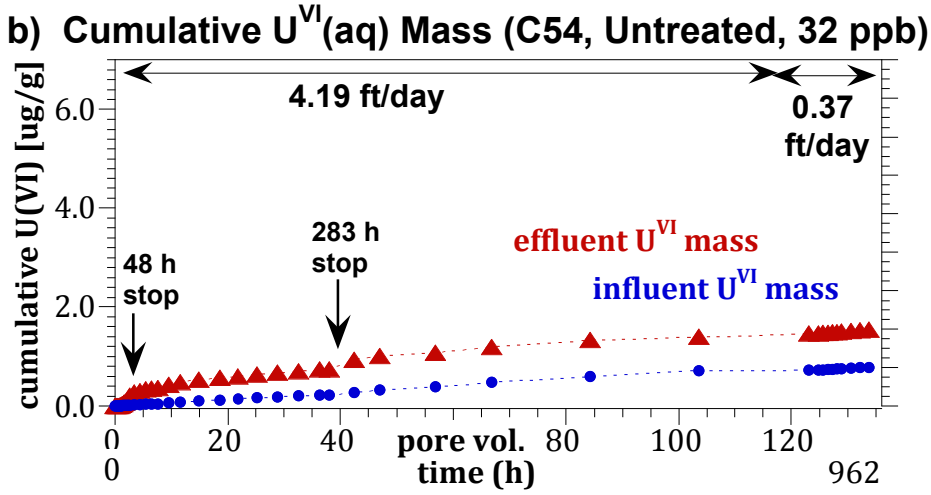

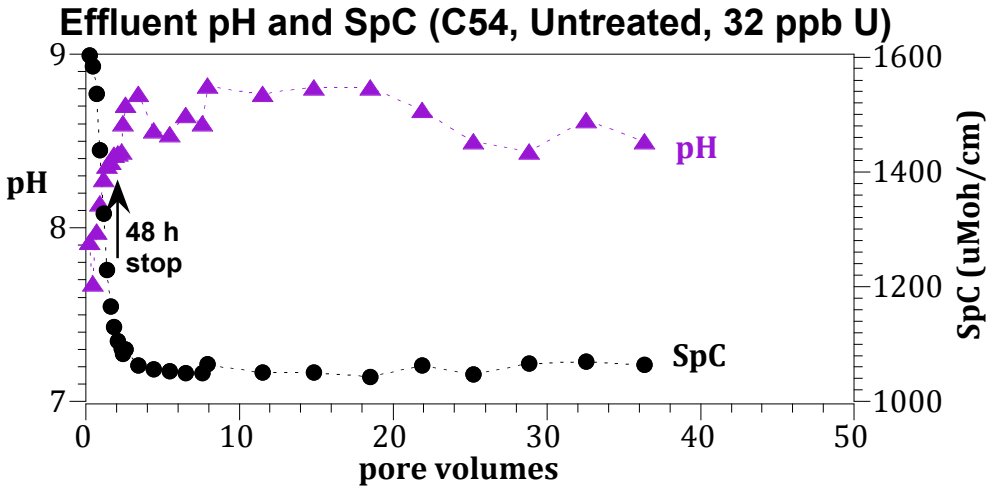

Column Experiment C55

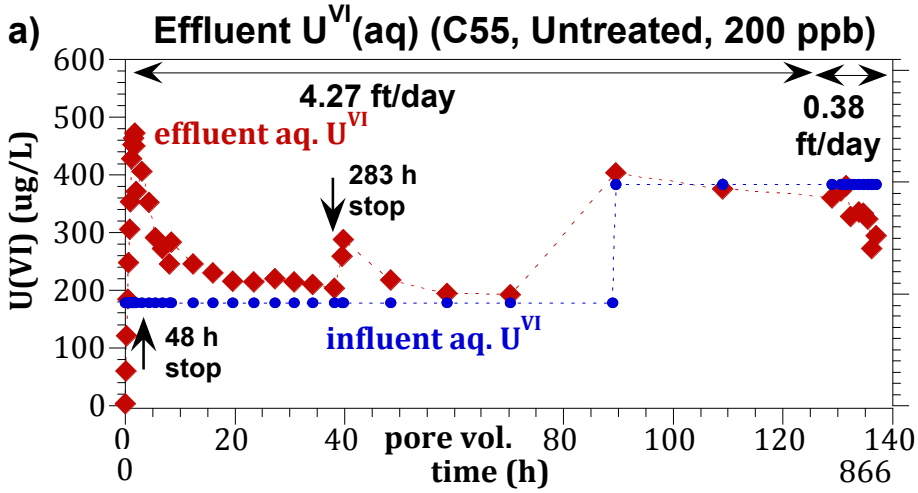

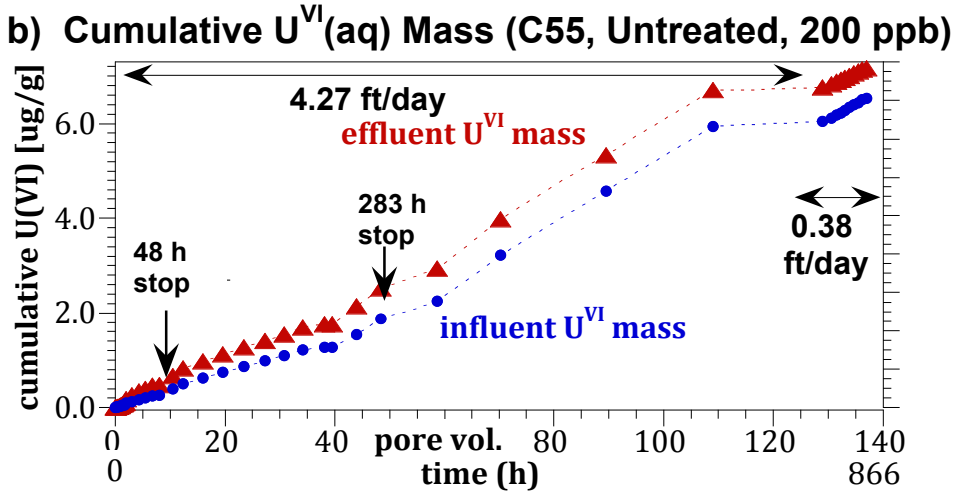

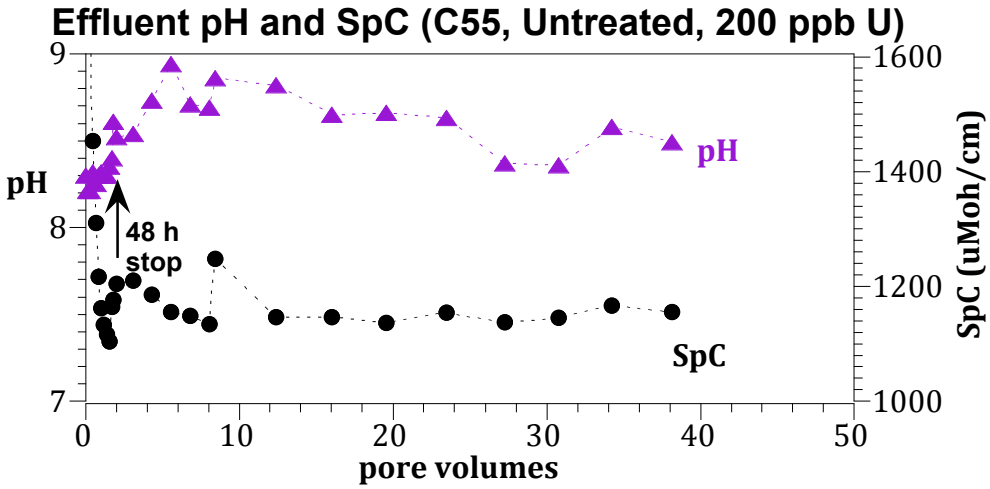

Column Experiment C56

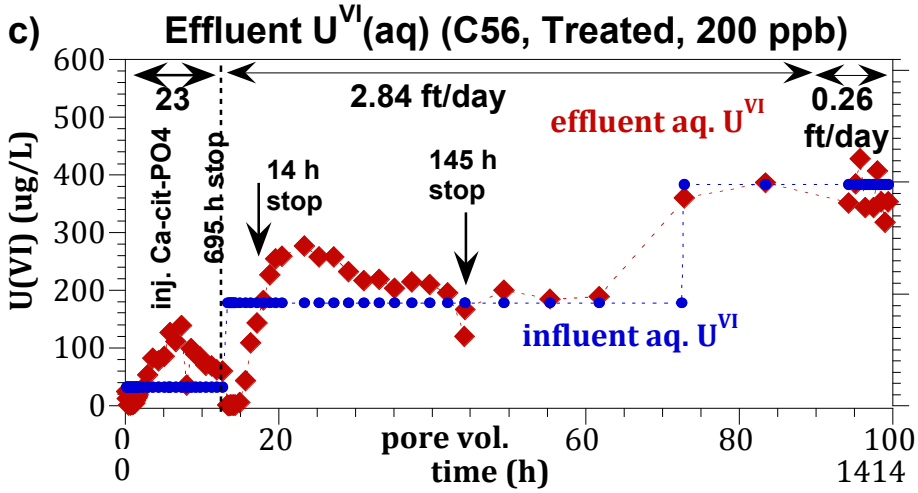

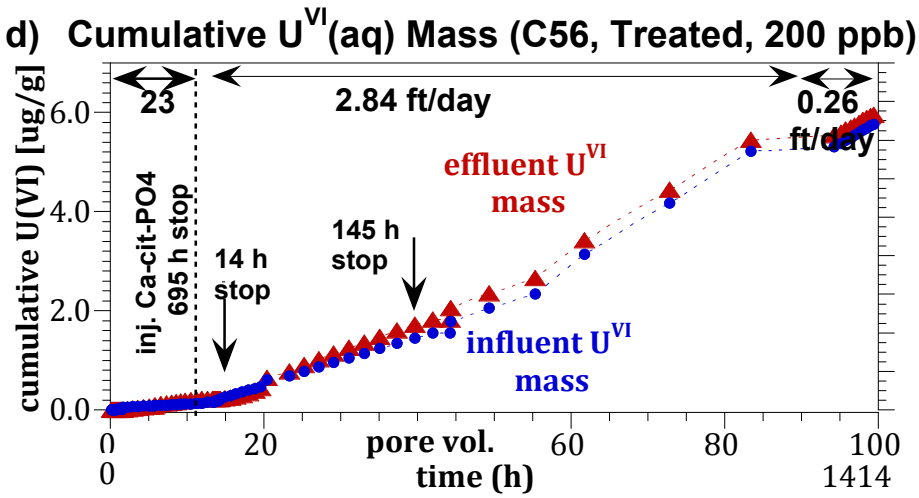

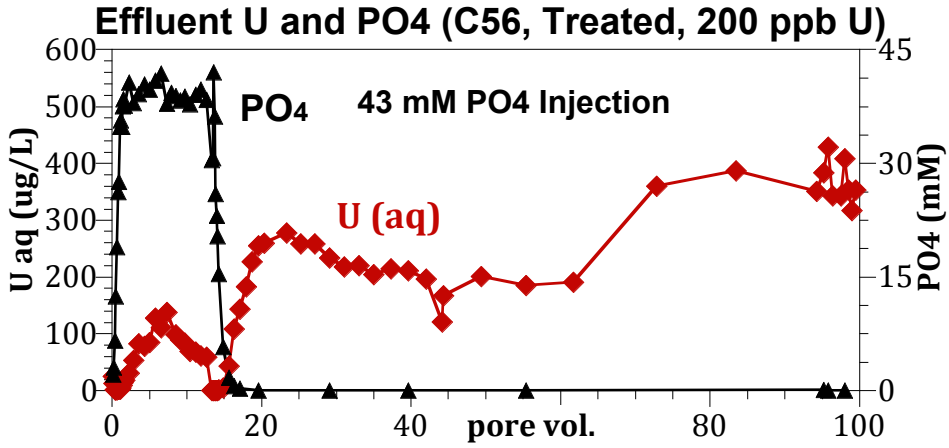

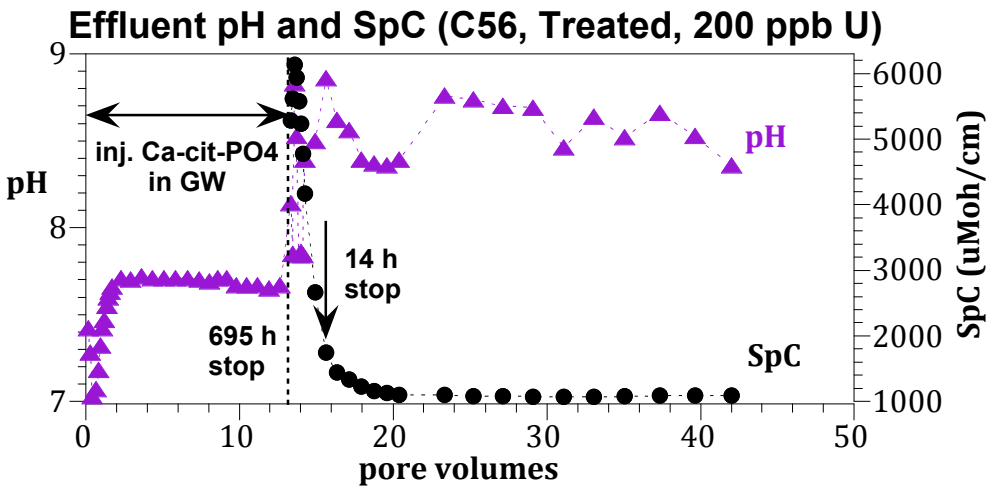
Effluent pH and SpC (C56, Treated, 200 ppb U)
pH
SpC (uMoh/cm)
pore volumes
inj. Ca-cit-PO4
in GW
14 h
stop
695 h
stop
pH
SpC
9
8
7
6000
5000
4000
3000
2000
1000
0
10
20
30
40
50

Column Experiment C57

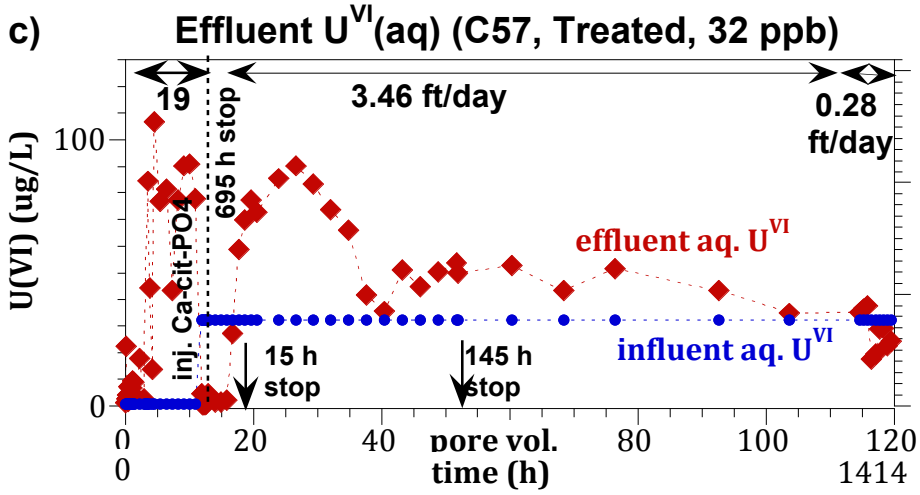

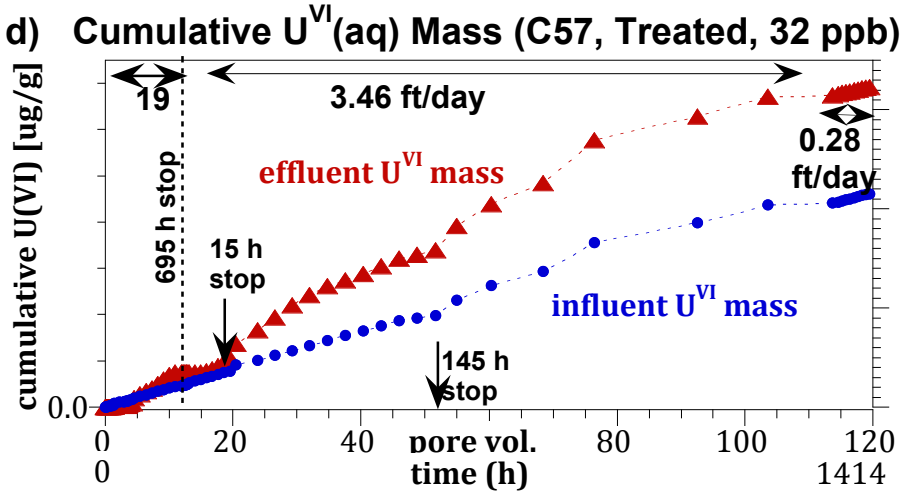

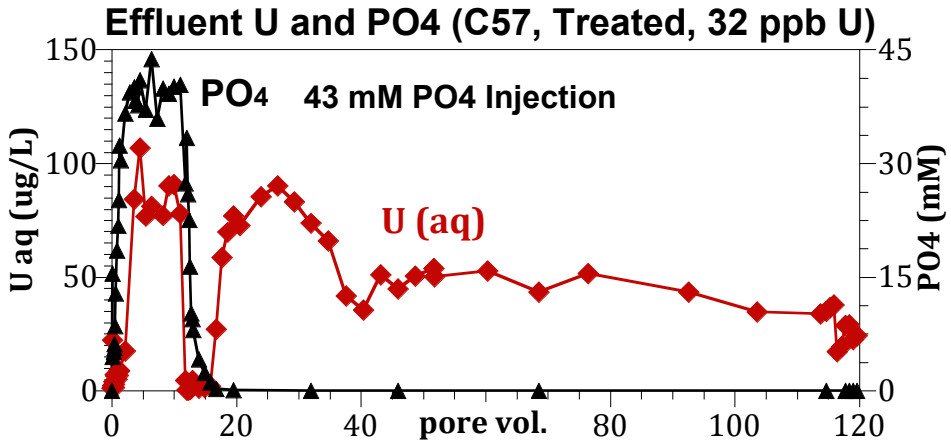

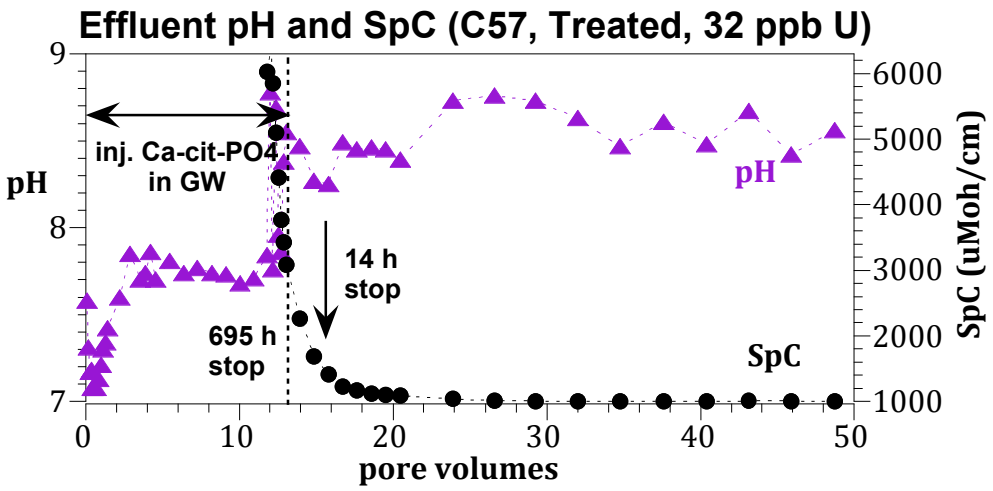
Effluent pH and SpC (C57, Treated, 32 ppb U)
pH
SpC (uMoh/cm)
pore volumes
inj. Ca-cit-PO4
in GW
14 h
stop
695 h
stop
pH
SpC
9
8
7
6000
5000
4000
3000
2000
1000
0
10
20
30
40
50

Column Experiment C58

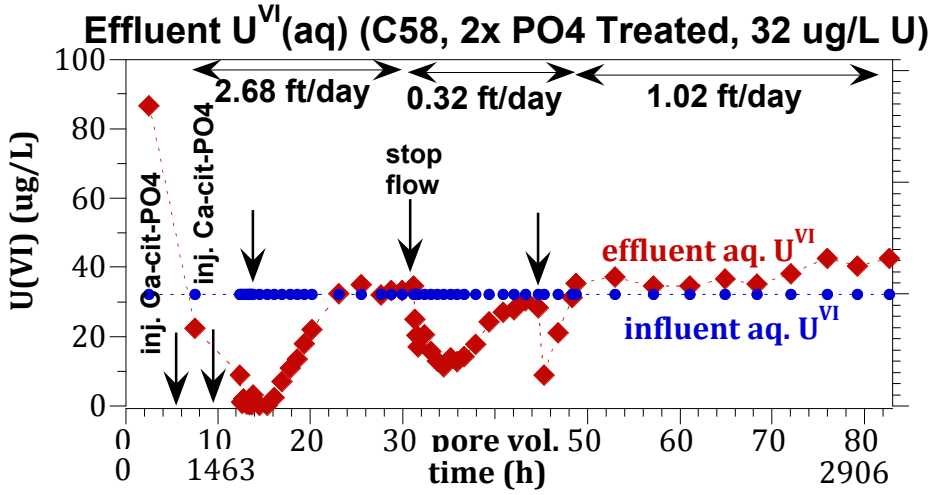

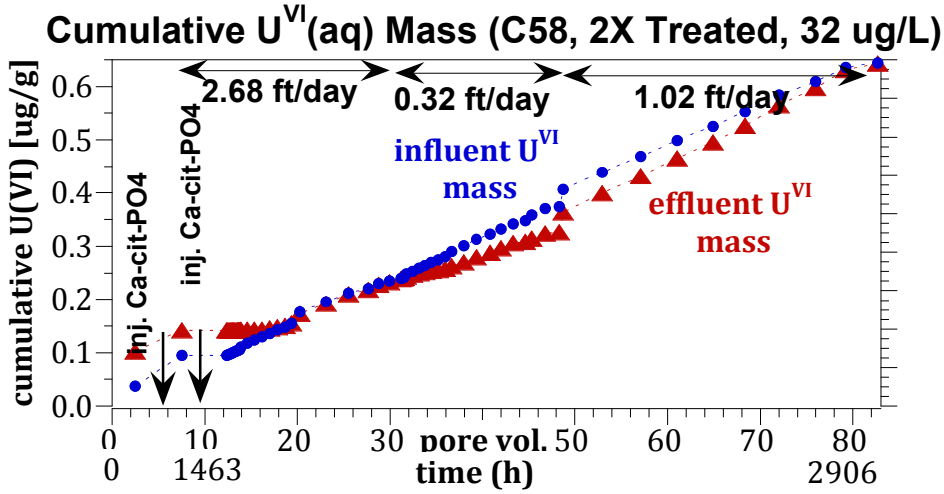

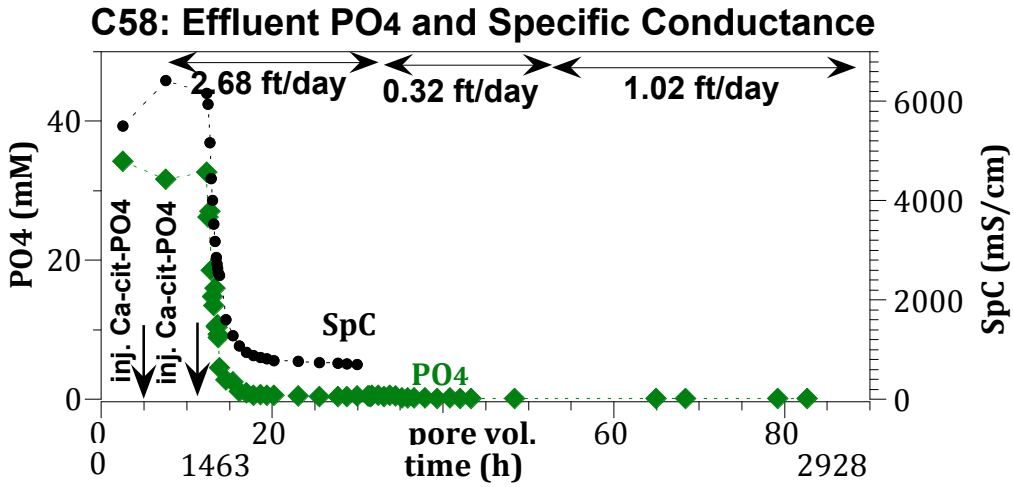

Column Experiment C59

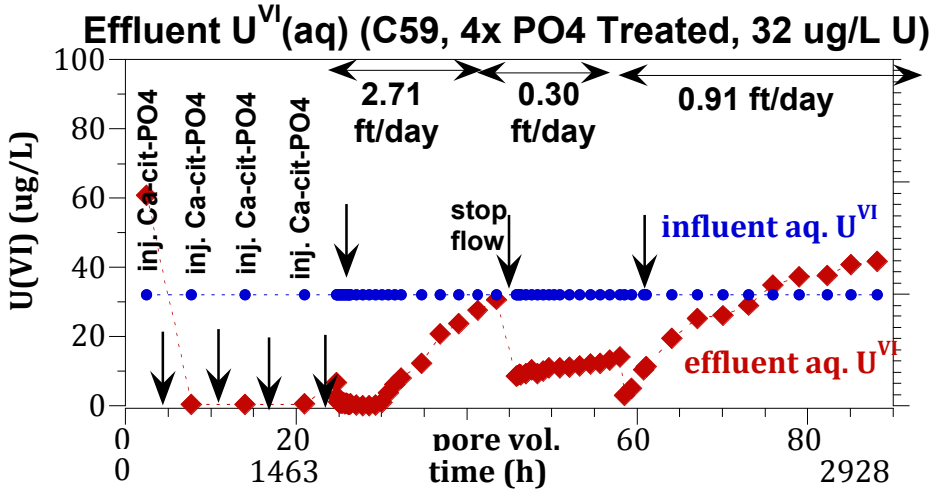

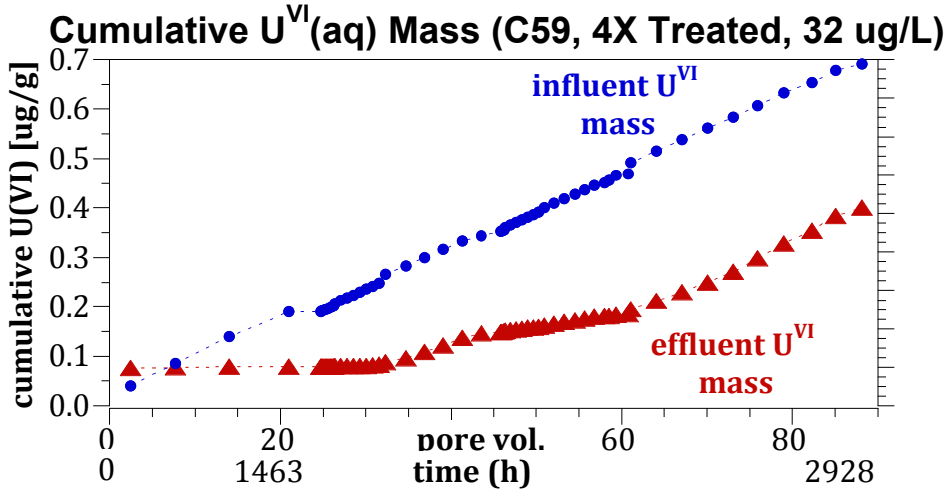

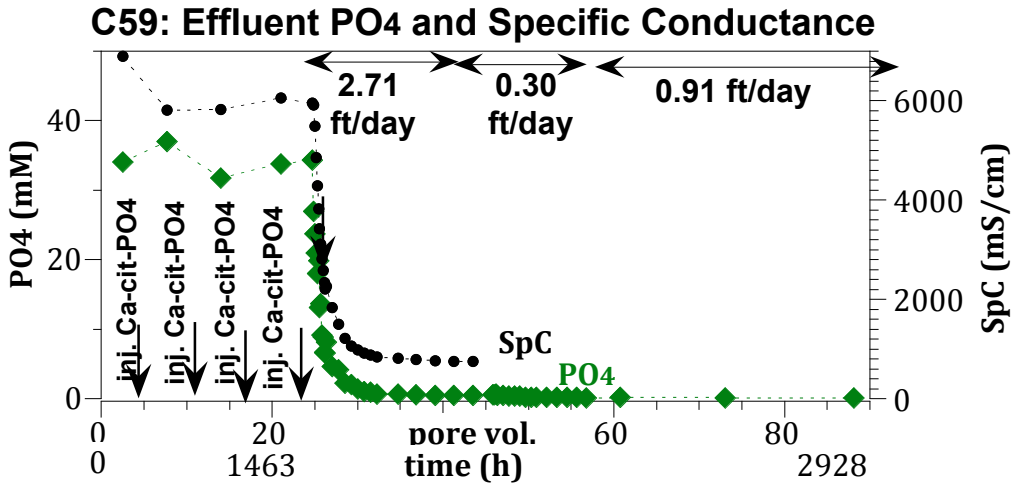

Appendix B

Uranium Extraction Results

Appendix B

Uranium Extraction Results

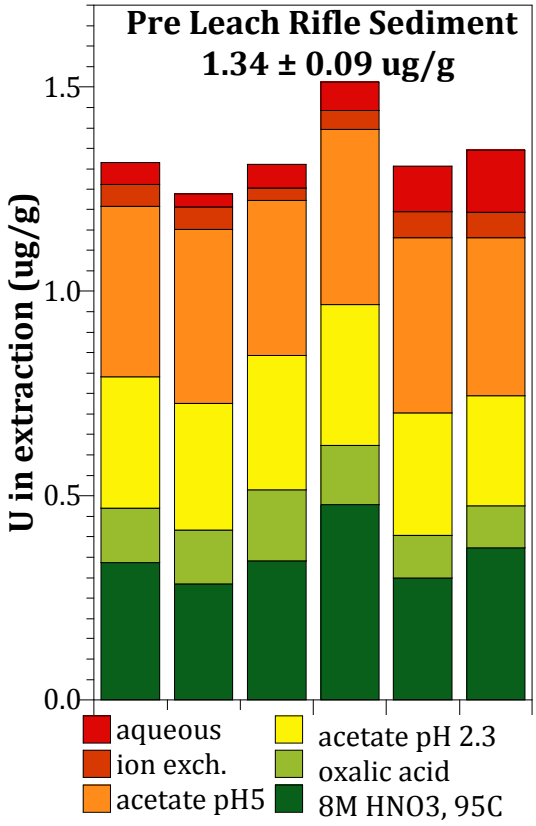

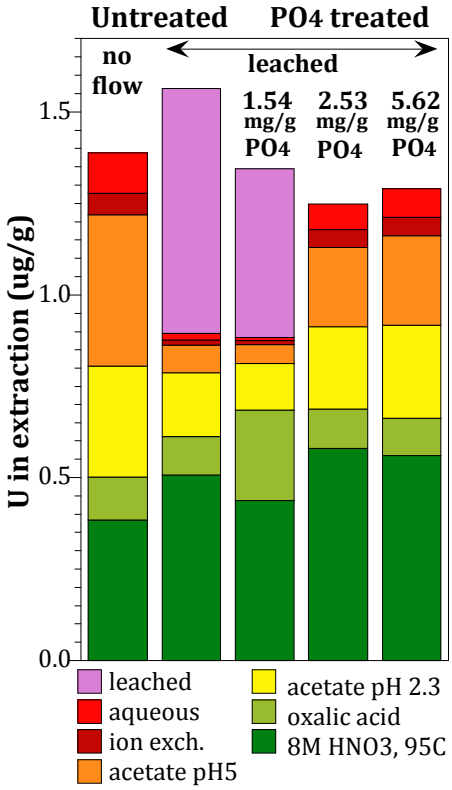

Table B.1. Selected uranium extractions on sediments and column uranium mass balance

#	PO4 treatment	U(VI) aqueous (ug/g)	U(VI) adsorbed (ug/g)	U(VI) acetate (ug/g)	U(VI) acetic acid (ug/g)	U(VI) oxalate (ug/g)	U(VI) 8M HNO3 (ug/g)	U(VI) total (ug/g)	U(VI) influent (ug/g)	U(VI) effluent (ug/g)	U(VI) net leached (ug/g)
no flow	none	0.111 ± 0.042	0.0576 ± 0.0094	0.414 ± 0.024	0.304 ± 0.038	0.117 ± 0.023	0.384 ± 0.090	1.388 ± 0.109	--	--	--
C55	none	0.0515 ± 0.0003	0.0516 ± 0.0012	0.190 ± 0.016	0.314 ± 0.024	0.150 ± 0.018	0.317 ± 0.011	1.075 ± 0.071	7.611	8.345	0.735
C56	1 x 45 mM	0.0690 ± 0.0367	0.0527 ± 0.0046	0.157 ± 0.025	0.303 ± 0.115	0.124 ± 0.029	0.555 ± 0.198	1.260 ± 0.482	6.709	6.928	0.220
C54	none	0.0179 ± 0.0049	0.142 ± 0.0007	0.0754 ± 0.0029	0.176 ± 0.010	0.104 ± 0.0102	0.385 ± 0.071	0.772 ± 0.0981	0.907	1.582	0.893
C57	1 x 45 mM	0.0085 ± 0.0010	0.0112 ± 0.0001	0.0524 ± 0.0046	0.128 ± 0.0014	0.247 ± 0.240	0.437 ± 0.0054	0.884 ± 0.250	1.074	1.610	0.536
C58	2 x 45 mM	0.0700 ± 0.0151	0.0487 ± 0.0159	0.0216 ± 0.0291	0.226 ± 0.0291	0.107 ± 0.0455	0.580 ± 0.214	1.248 ± 0.426	0.750	0.748	-0.002
C59	4 x 45 mM	0.0775 ± 0.0234	0.0510 ± 0.0055	0.244 ± 0.0209	0.254 ± 0.0200	0.103 ± 0.0039	0.560 ± 0.0664	1.289 ± 0.0116	0.804	0.467	-0.337

Appendix C

Comparison of Leaching Results

Appendix C

Comparison of Leaching Results

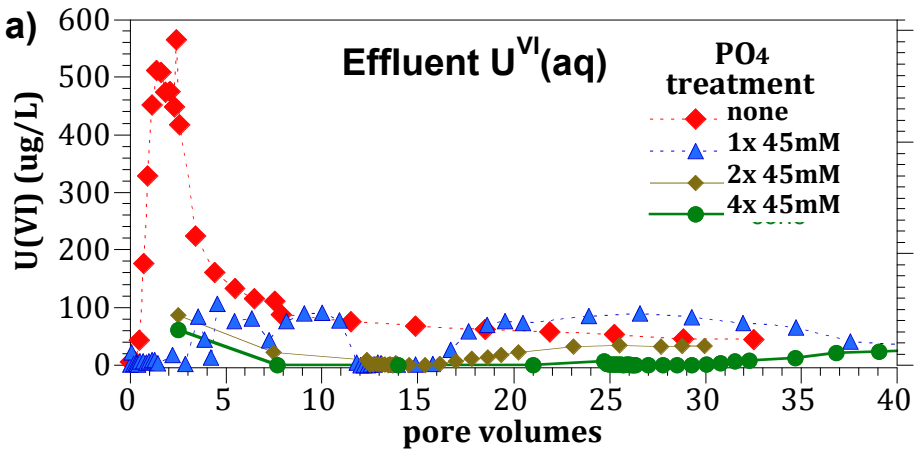

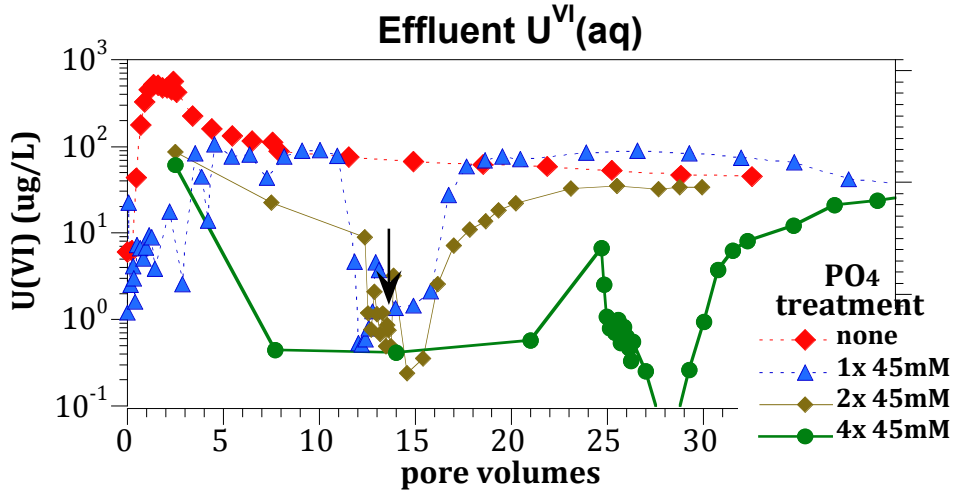

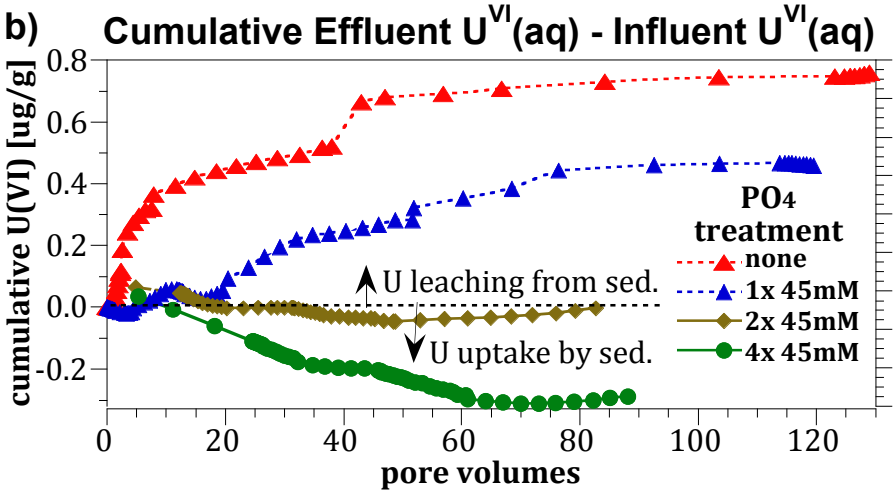
b)
Cumulative Effluent U^VI(aq) - Influent U^VI(aq)
cumulative U(VI) [ug/g]
0.8
0.6
0.4
0.2
0.0
-0.2
0
20
40
60
80
100
120
pore volumes
PO4 treatment
none
1x 45mM
2x 45mM
4x 45mM
U leaching from sed.
U uptake by sed.

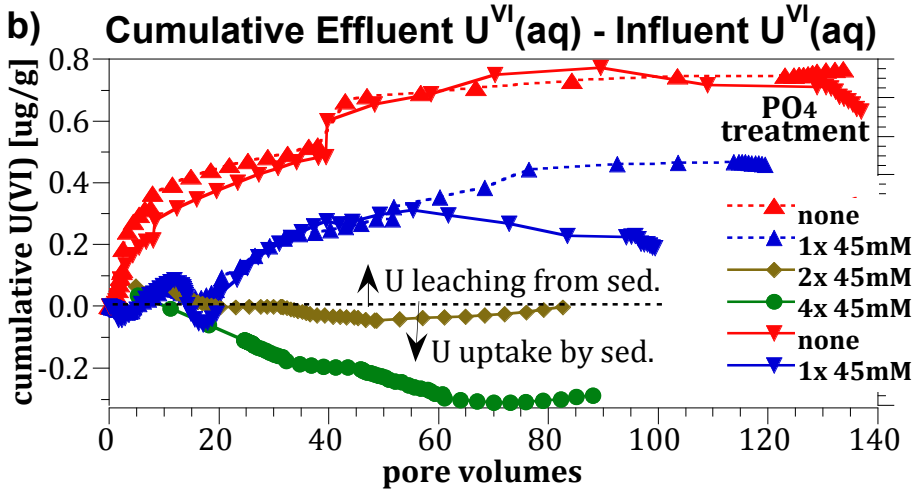
b)
Cumulative Effluent U^VI(aq) - Influent U^VI(aq)
cumulative U(VI) [ug/g]
0.8
0.6
0.4
0.2
0.0
-0.2
0
20
40
60
80
100
120
140
pore volumes
PO4 treatment
none
1x 45mM
2x 45mM
4x 45mM
none
1x 45mM
U leaching from sed.
U uptake by sed.

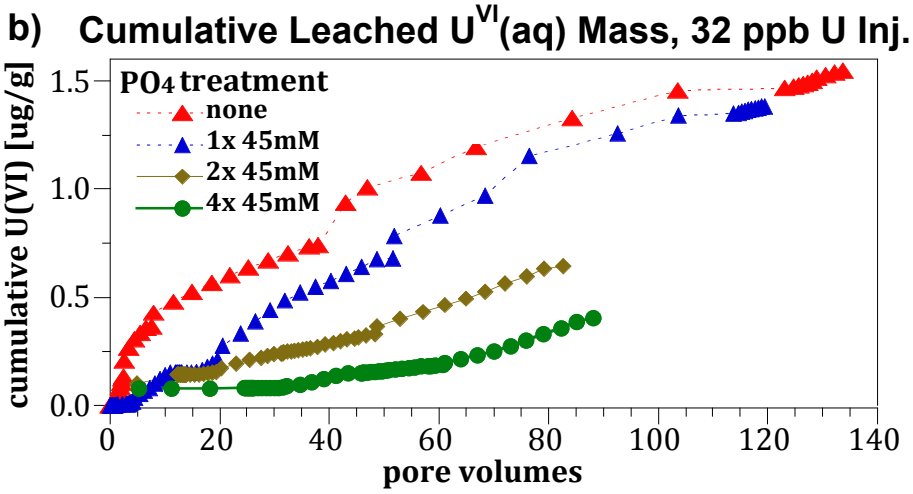
b)
Cumulative Leached U^VI(aq) Mass, 32 ppb U Inj.
cumulative U(VI) [ug/g]
1.5
1.0
0.5
0.0
0
20
40
60
80
100
120
140
pore volumes
PO4 treatment
none
1x 45mM
2x 45mM
4x 45mM

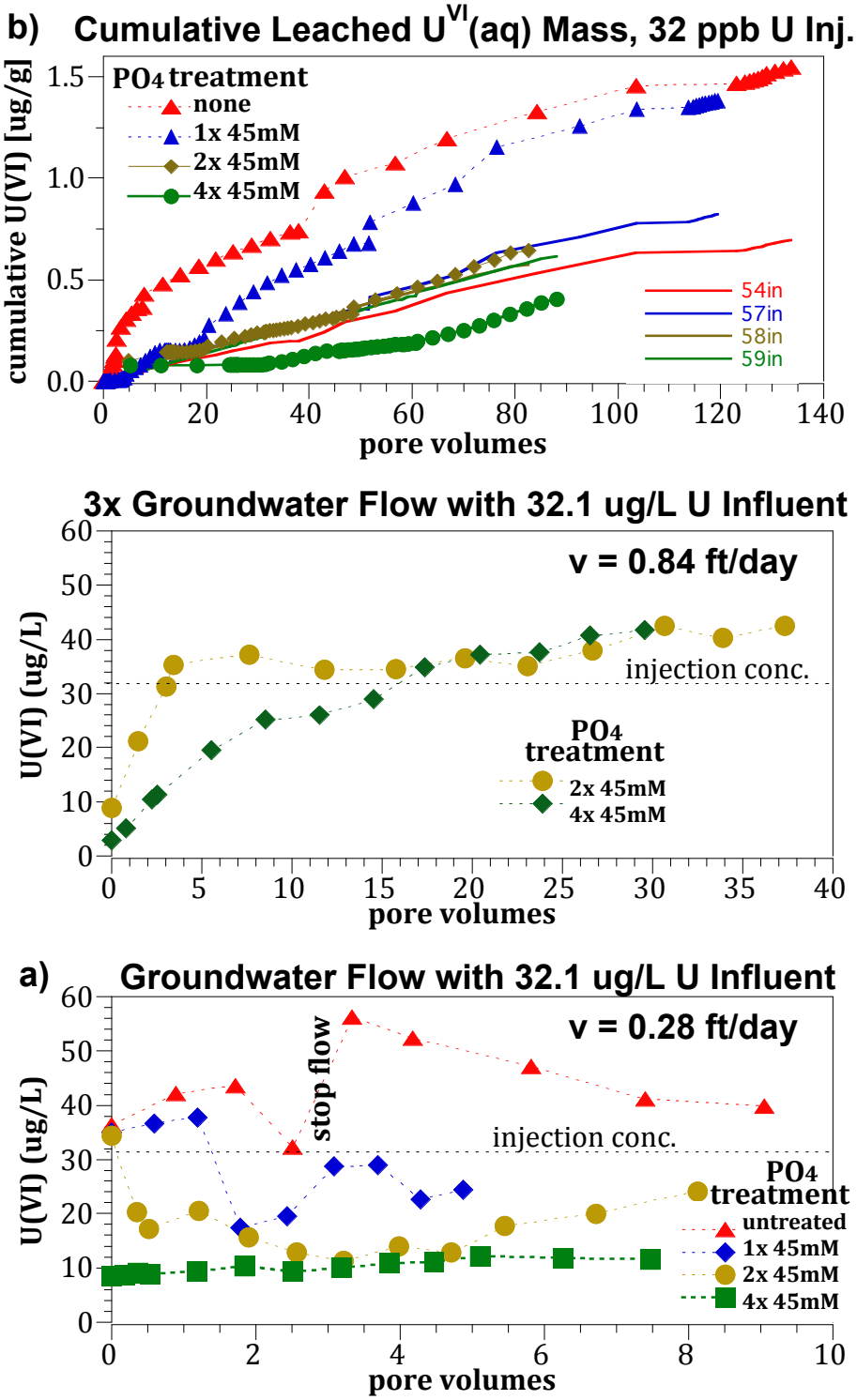
b) Cumulative Leached U^VI(aq) Mass, 32 ppb U Inj.
cumulative U(VI) [ug/g]
PO4 treatment
none
1x 45mM
2x 45mM
4x 45mM
54in
57in
58in
59in
pore volumes
3x Groundwater Flow with 32.1 ug/L U Influent
v = 0.84 ft/day
U(VI) (ug/L)
injection conc.
PO4 treatment
2x 45mM
4x 45mM
pore volumes
a) Groundwater Flow with 32.1 ug/L U Influent
v = 0.28 ft/day
stop flow
U(VI) (ug/L)
injection conc.
PO4 treatment
untreated
1x 45mM
2x 45mM
4x 45mM
pore volumes

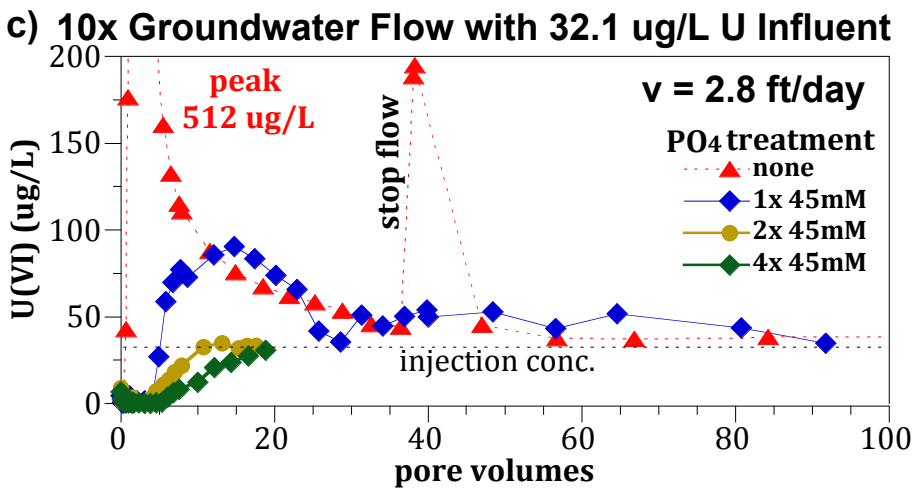
c) 10x Groundwater Flow with 32.1 ug/L U Influent
peak
512 ug/L
stop flow
v = 2.8 ft/day
PO4 treatment
none
1x 45mM
2x 45mM
4x 45mM
injection conc.
U(VI) (ug/L)
pore volumes

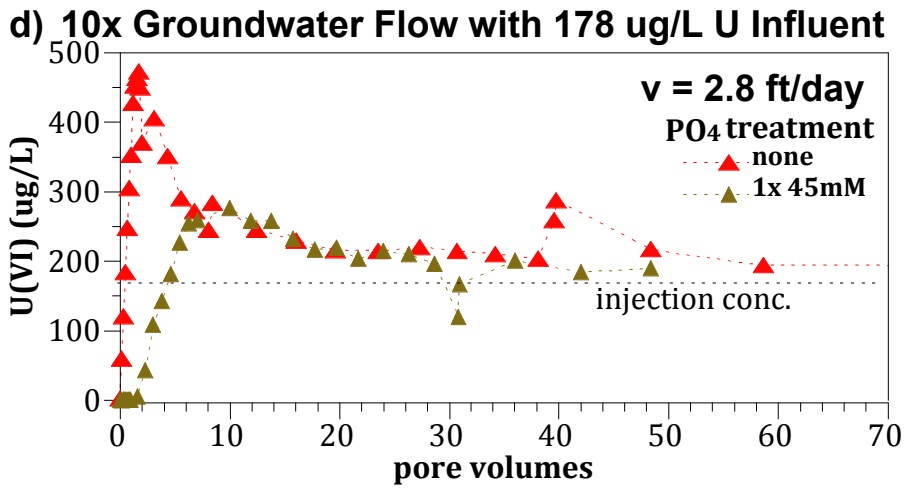
d) 10x Groundwater Flow with 178 ug/L U Influent
v = 2.8 ft/day
PO4 treatment
none
1x 45mM
injection conc.
U(VI) (ug/L)
pore volumes

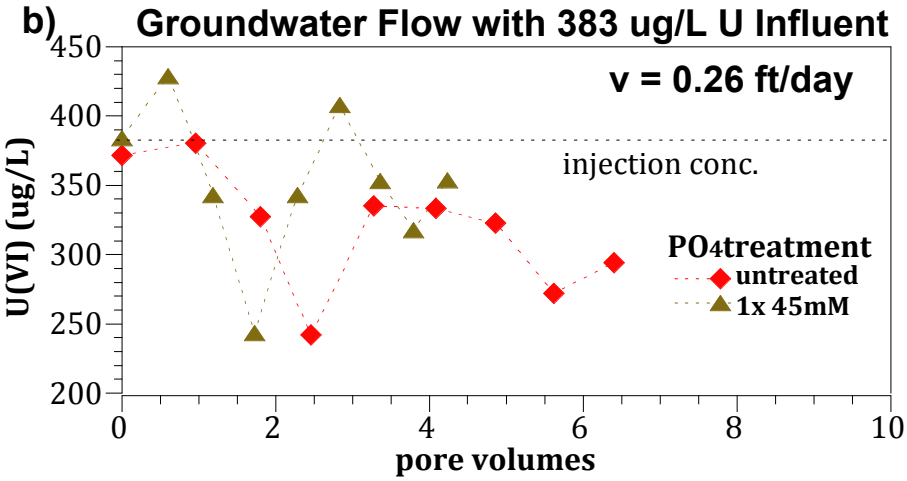
b) Groundwater Flow with 383 ug/L U Influent
v = 0.26 ft/day
injection conc.
PO4treatment
untreated
1x 45mM
U(VI) (ug/L)
pore volumes

Appendix D

Uranium Release Rates and Phosphate Concentration

Appendix D

Uranium Release Rates and Phosphate Concentration

Table D.1. Uranium(VI) release rates calculated during continuous flow in columns

#	PO4 treatment	U(VI) inject conc. (ug/L)	Flow Rate (ft/day)	U(VI) effluent (ug/L)	U(VI) rel. rate* (ug/Kg/day)
C55	none	178.85	4.27	213.5	63.7
		383.4	0.383	380.2	-0.56
C56	1 x 45 mM	178.85	2.84	214.7	2.20
		383.4	0.258	349.2	-5.71
C54	none	32.1	4.19	38.51	14.6
		32.1	0.371	43.49	2.25
C57	1 x 45 mM	32.1	3.46	44.85	14.1
		32.1	0.283	17.42	-4.85
C58	2 x 45 mM	32.1	2.68	33.1	-16.7
		32.1	0.822	21.21	-9.85
		32.1	0.32	4.97	-4.43
C59	4 x 45 mM	32.1	2.71	21.85	-36.5
		32.1	0.813	11.1	-13.9
		32.1	0.298	8.93	-3.77

* + is U release from sed., - is U uptake by sed.

Table D.2. Uranium(VI) release rates calculated during stop flows in columns

#	PO4 treatment	stop (pore vol)	U(VI) stop conc. (ug/L)	U(VI) start conc. (ug/L)	U(VI) rel. rate* (ug/Kg/day)
C55	none	2.0	450.5	371.2	-8.60
		39.6	204.1	259.4	1.01
C56	1 x 45 mM	14.6	0.74	1.33	0.30
		44.2	196.3	120.3	-3.99
C54	none	2.4	448.2	564.6	13.3
		38.0	44.40	188.6	2.80
C57	1 x 45 mM	14.6	4.59	3.73	-0.416
		44.2	50.44	53.9	0.174
C58	2 x 45 mM	13.8	0.48	3.20	1.39
		29.9	33.36	34.5	0.065
		44.6	33.21	9.54	-0.513
C59	4 x 45 mM	11.5	0.33	0.55	0.109
		43.5	30.70	8.51	-1.228
		58.00	14.71	2.95	-0.246

* + is U release from sed., - is U uptake by sed.

Table D.3. Uranium(VI) release rates calculated during phosphate injections in columns

#	PO4 treatment	stop (pore vol)	U(VI) stop conc. (ug/L)	U(VI) start conc. (ug/L)	U(VI) rel. rate* (ug/Kg/day)
C56	1 x 45 mM	12.6	59.4	0.70	-29.5
C57	1 x 45 mM	11.8	77.8	4.67	-35.4
C58	2 x 45 mM	4.95	32.1	86.5	1.19
		12.3	32.1	0.44	-0.002
C59	4 x 45 mM	5.3	32.1	3.32	-0.609
		11.2	32.1	0.44	-1.23
		18.2	32.1	0.41	-0.572
		24.6	32.1	0.57	-0.285

* + is U release from sed., - is U uptake by sed.

Table D.4. Calculated phosphate precipitate in sediment based on measured phosphate influent and effluent concentrations in columns

#	injection U conc. (ug/L)	number of PO_4 injections	PO_4 injected (mmol)	PO_4 effluent (mmol)	PO_4 in sed. (mg/g)
C57	32.1	1	17.336	15.764	1.558
C56	383	1	14.107	12.588	1.541
C58	32.1	2	15.858	12.751	2.865
C59	32.1	4	31.793	25.878	5.956

Table D.5. Column Physical Parameters

#	dry sed. (g)	pore vol. (mL)	dry bulk density (g/cm3)	porosity (cm3/cm3)
C54	102.657	23.463	1.578	0.3606
C55	103.247	22.313	1.587	0.3430
C56	95.804	30.456	1.473	0.4681
C57	93.628	28.682	1.439	0.4408
C58	102.982	25.238	1.583	0.3879
C59	100.005	23.675	1.537	0.3639

Table D.6. Cumulative U(VI) Leached Mass

#	PO4 treatment	U(VI) inject conc. (ug/L)	U(VI) Influent (ug/g)	U(VI) effluent (ug/g)	Net Leached U(VI) (ug/g)
C55	none	179, 383	7.611	8.345	0.735
C56	1 x 45 mM	179, 383	6.709	6.928	0.220
C54	none	32.1	0.907	1.800	0.893
C57	1 x 45 mM	32.1	1.074	1.610	0.536
C58	2 x 45 mM	32.1	0.750	0.748	-0.002
C59	4 x 45 mM	32.1	0.804	0.467	-0.337

* + is U release from sed., - is U uptake by sed.

Table D.7. Uranium adsorption calculated from breakthrough curves

#	PO4 treatment	U(VI) inject conc. (ug/L)	U(VI) Rf	U(VI) K_d (cm^3/g)
C55	none	179, 383	6.80	1.33
C56	1 x 45 mM	179, 383	4.16	0.68
C54	none	32.1	7.10	1.94
C57	1 x 45 mM	32.1	5.82, 2.70	1.48, 0.52
C58	2 x 45 mM	32.1	6.92, 7.20	1.45, 1.52
C59	4 x 45 mM	32.1	10.9, 7.50	2.35, 1.54

Appendix E

Phosphate Concentration and U Mobility

Appendix E

Phosphate Concentration and U Mobility

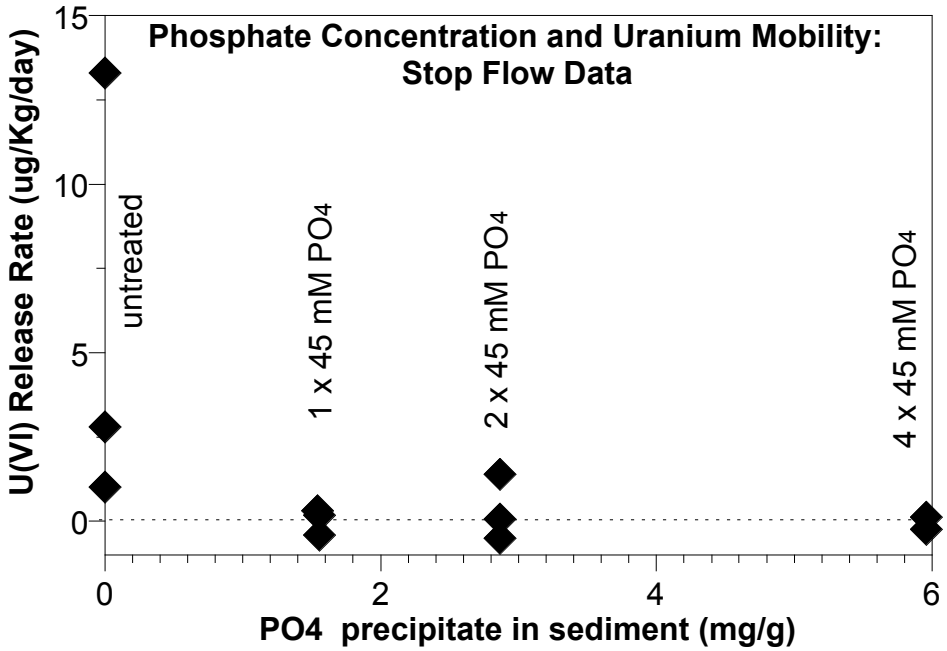

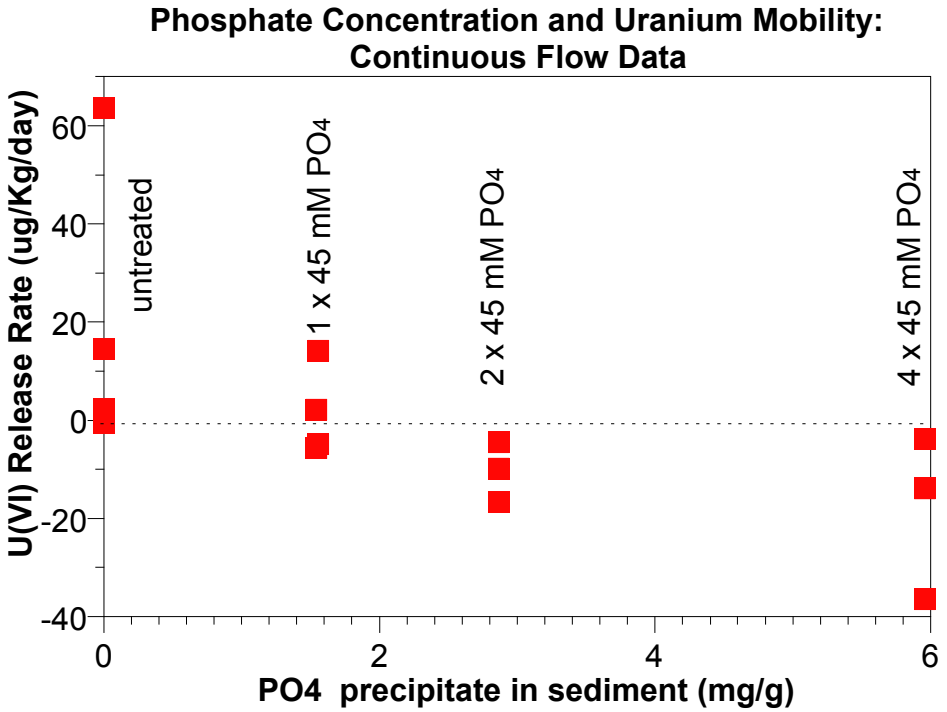

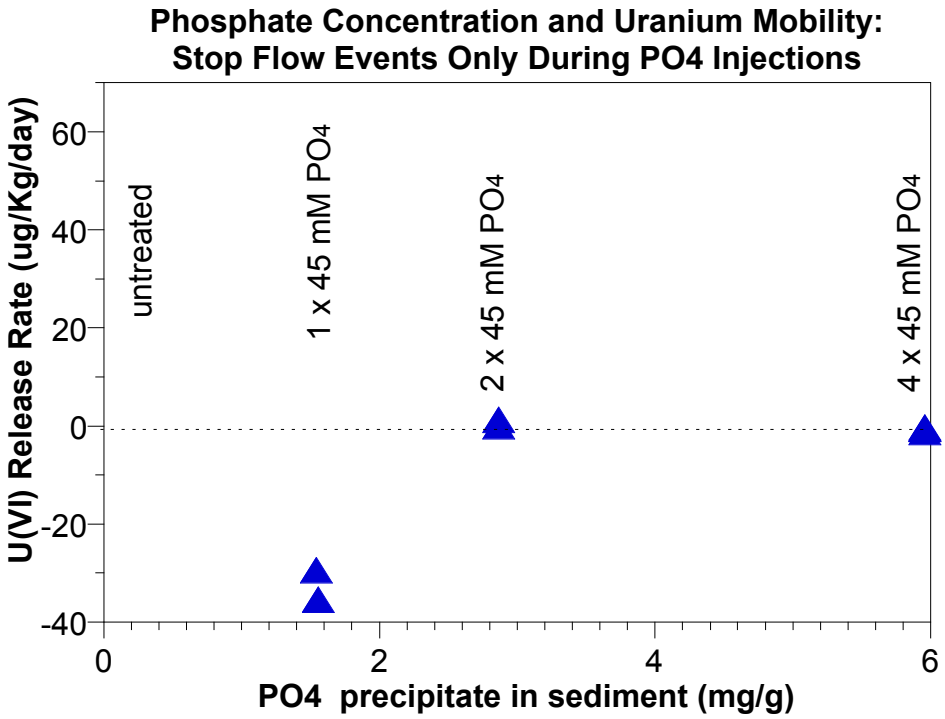
Phosphate Concentration and Uranium Mobility:
Stop Flow Events Only During PO4 Injections
U(VI) Release Rate (ug/Kg/day)
60
40
20
0
-20
-40
untreated
1 x 45 mM PO4
2 x 45 mM PO4
4 x 45 mM PO4
0
2
4
6
PO4 precipitate in sediment (mg/g)

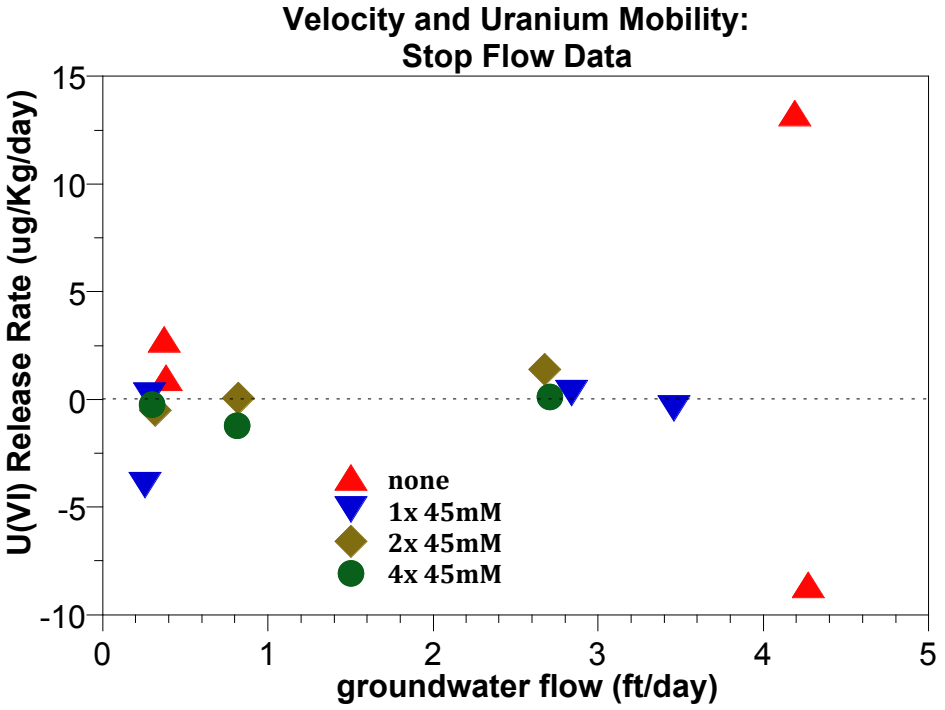
Velocity and Uranium Mobility:
Stop Flow Data
U(VI) Release Rate (ug/Kg/day)
15
10
5
0
-5
-10
none
1x 45mM
2x 45mM
4x 45mM
0
1
2
3
4
5
groundwater flow (ft/day)

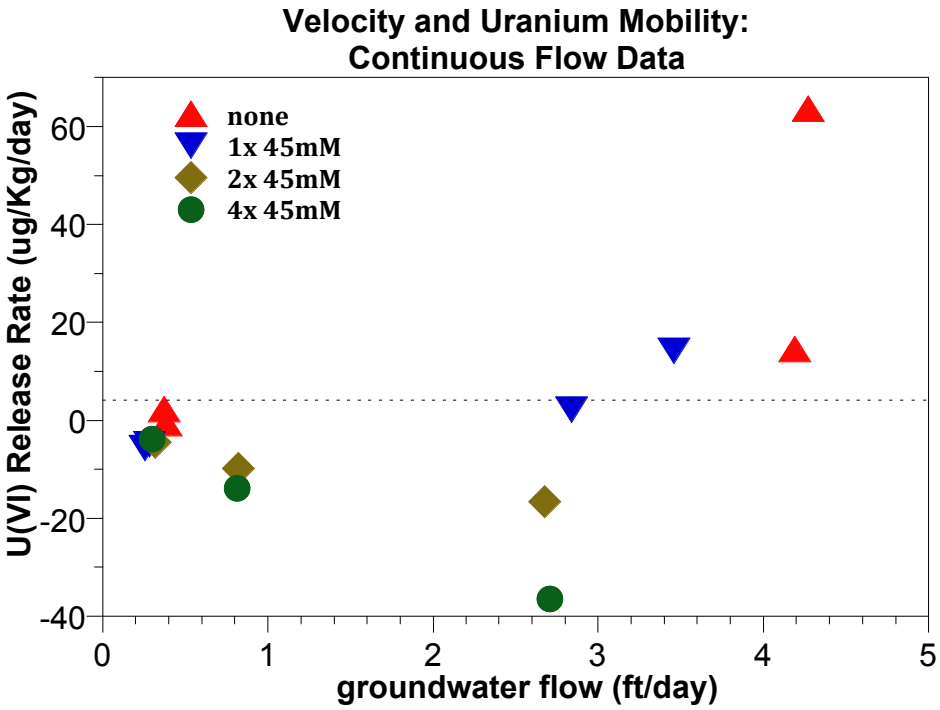
Velocity and Uranium Mobility:
Continuous Flow Data
none
1x 45mM
2x 45mM
4x 45mM
U(VI) Release Rate (ug/Kg/day)
60
40
20
0
-20
-40
0
1
2
3
4
5
groundwater flow (ft/day)

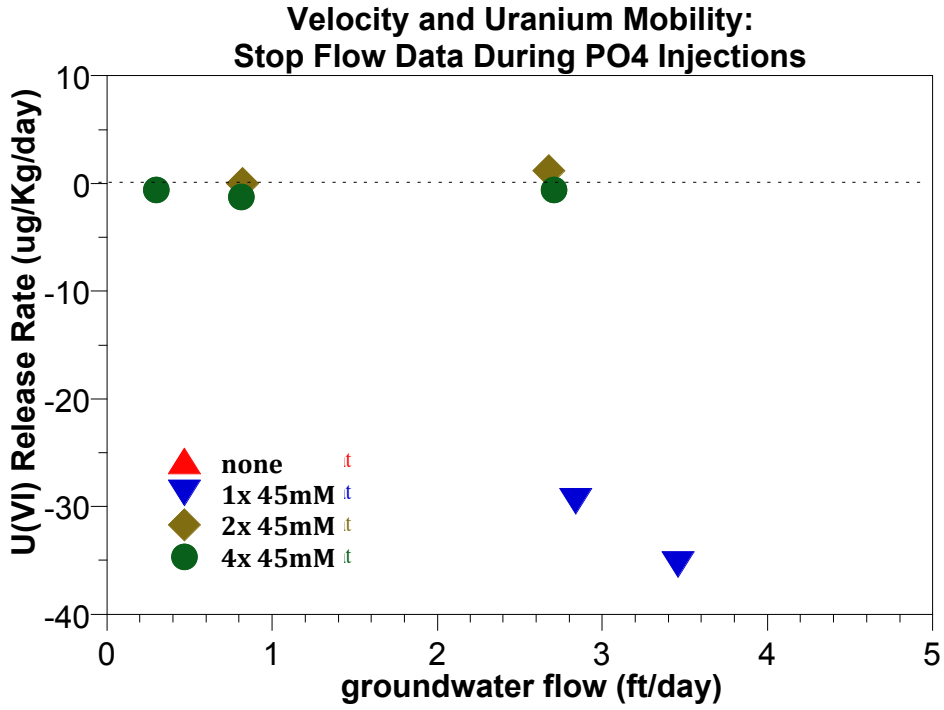
Velocity and Uranium Mobility:
Stop Flow Data During PO4 Injections
none
1x 45mM
2x 45mM
4x 45mM
U(VI) Release Rate (ug/Kg/day)
10
0
-10
-20
-30
-40
0
1
2
3
4
5
groundwater flow (ft/day)

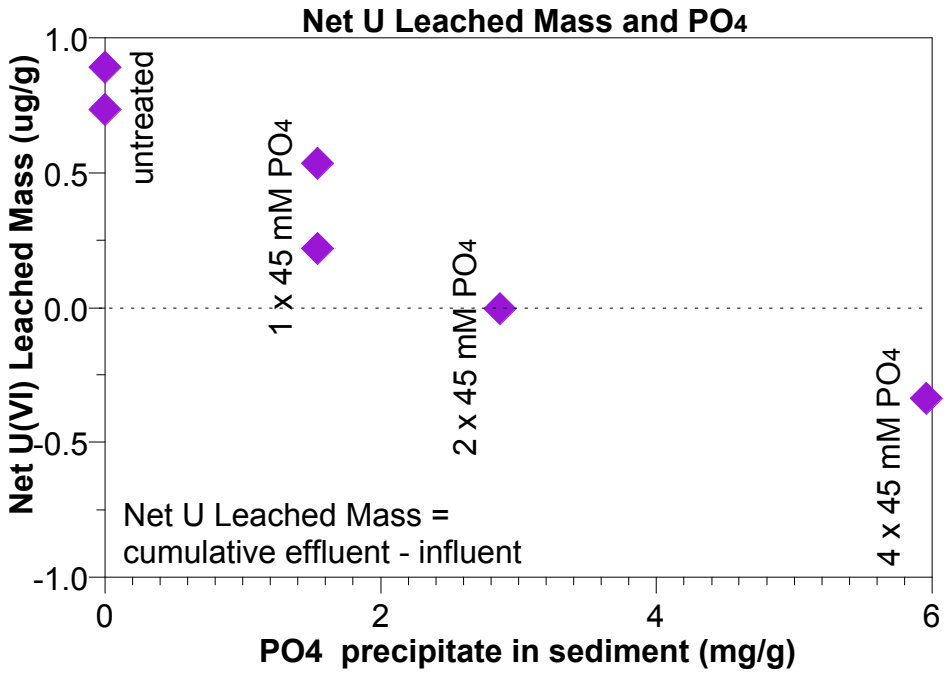
Net U Leached Mass and PO4
Net U(VI) Leached Mass (ug/g)
1.0
0.5
0.0
-0.5
-1.0
untreated
1 x 45 mM PO4
2 x 45 mM PO4
4 x 45 mM PO4
Net U Leached Mass =
cumulative effluent - influent
0
2
4
6
PO4 precipitate in sediment (mg/g)

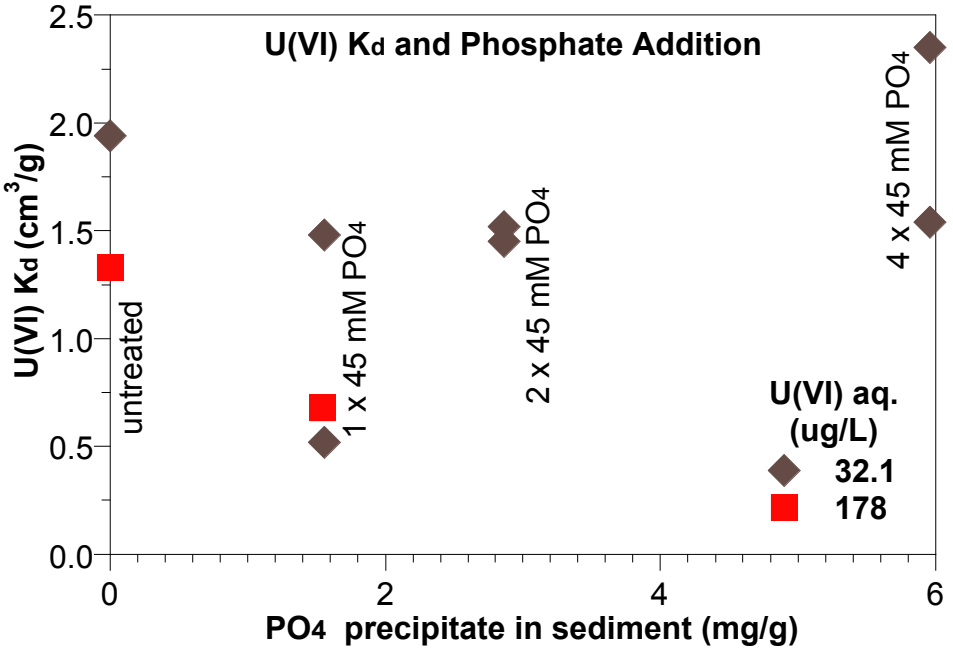
U(VI) Kd and Phosphate Addition
U(VI) Kd (cm3/g)
2.5
2.0
1.5
1.0
0.5
0.0
untreated
1 x 45 mM PO4
2 x 45 mM PO4
4 x 45 mM PO4
U(VI) aq.
(ug/L)
32.1
178
0
2
4
6
PO4 precipitate in sediment (mg/g)

Distribution

No. of Copies	
4	Mark Rigali Sandia National Laboratories Applied Systems Analysis and Research Department PO Box 58000, MS 0747 Albuquerque, NM 87185-0747

No. of Copies		
2	**Local Distribution** Pacific Northwest National Laboratory	
1	Szecsody JE	P7-59
1	Vermeul VR	K4-18

Pacific Northwest
NATIONAL LABORATORY

Proudly Operated by **Battelle** *Since 1965*

U.S. DEPARTMENT OF
ENERGY

902 Battelle Boulevard
P.O. Box 999
Richland, WA 99352
1-888-375-PNNL (7665)

www.pnnl.gov